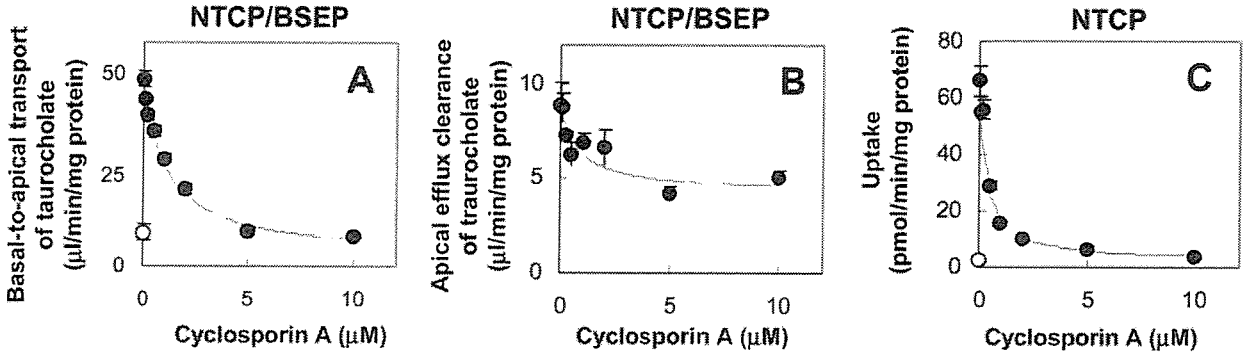

FIG. 4. Inhibition of the transport of taurocholate by cyclosporin A. Various concentrations of cyclosporin A were added to the apical and basal compartment of LLC-NTCP/BSEP (A and B). After 30 min, the inhibitory effects of cyclosporin A (closed circles) and an excess (500 μM) of taurocholate (open circle) on the basal-to-apical transport of [^{3}H]taurocholate (1 μM) for 1 h across LLC-NTCP/BSEP cell monolayers were studied (A). Apical efflux clearance PS3 of taurocholate was calculated versus the intracellular concentration of taurocholate determined at the end of the experiments (B). The inhibitory effects of cyclosporin A (closed circles) and an excess (500 μM) of taurocholate (open circle) on the uptake of [^{3}H]taurocholate (1 μM) for 1 min into LLC-NTCP cells were studied (C).

the uptake of taurocholate by rat Ntcp to 60% of the total uptake (Fattinger et al., 2000). However, in this study, after incubation with 100 μM rifampicin and rifamycin SV, the reduction in C_{cell} was not as much as 60%. An increase by rifampicin and only a slight decrease by rifamycin SV were observed (Fig. 3). If we hypothesize there is no species difference in the inhibitory effect of these drugs between humans and rats, this result indicates that the inhibition of NTCP and BSEP balanced each other.

Captopril and cimetidine are reported to cause cholestasis (Mohiud-din and Lewis, 2004). However, their interactions with bile acid transporters have not been reported [cimetidine does not have a significant inhibitory effect on BSEP (Wang et al., 2003)], and other pathways are postulated as a possible mechanism. Corresponding to this, both captopril and cimetidine did not affect the transcellular transport and C_{cell} of taurocholate at 100 μM (Fig. 3, A–C).

The inhibitory effect of cyclosporin A, an inhibitor of both NTCP and BSEP, was also examined as well as the inhibition kinetics of the transcellular transport when both the uptake and efflux processes are affected (Fig. 4). The basal-to-apical transport clearance $PS_{b\text{-}a}$ was inhibited with a K_i value of 1.0 ± 0.2 (μM). The efflux clearance PS3 was inhibited depending on the medium concentration of cyclosporin A. Although estimation of the exact K_i value is difficult, it appeared to be close to the reported K_i value for the inhibition of the uptake of taurocholate into human BSEP-expressing membrane vesicles by cyclosporin A (9.5 μM) (Byrne et al., 2002)

The question that we must consider here is to what extent inhibition of the uptake and efflux process affects the net transcellular transport. It was estimated that the K_i value for the inhibitory effect of cyclosporin A on the uptake of taurocholate into human NTCP-expressing LLC-PK1 cells was 0.27 ± 0.06 (μM) (Fig. 4). This value is similar to the K_i value for $PS_{b\text{-}a}$, which suggests that the inhibition of $PS_{b\text{-}a}$ reflects the inhibition of the uptake process mediated by NTCP. Although we do not know whether NTCP or BSEP is important for the cyclosporin A-induced cholestasis in physiological situations, the result of this study and the following aspects support the importance of NTCP. The transcellular transport clearance can be expressed as the hybrid of each transmembrane transport clearance as described under *Data Analysis*: $PS_{b\text{-}a} = PS1 \cdot PS3/(PS2 + PS3)$. If the efflux clearance across the apical membrane, PS3, is far greater than that across the basal membrane, PS2, $PS_{b\text{-}a}$ is nearly equal to PS1. Thus, inhibition of the uptake process, PS1, can lead to inhibition of transcellular transport more easily than inhibition of the efflux process, PS3. The effect of inhibition of the uptake and/or efflux process on the net transcellular transport is simulated in Fig. 5. The ratio of PS2:PS3 is substituted by the measured value in the isolated rat liver perfusion studies: PS3, 69.2 ± 6.3 (μl/min/g liver); PS2, 8.4 ± 0.6 (μl/min/g liver) (Akita et al., 2002). If the efficacy of the inhibitory effect of the drug is similar for the uptake and efflux processes, inhibition of uptake is more effective than that of efflux as far as the net transcellular transport is concerned.

BSEP has been extensively studied as a target molecule of drug-induced cholestasis because it plays a role in the regulation of the concentration of bile acids in hepatocytes. Inhibition of BSEP leads to an intracellular accumulation of bile acids, resulting in cellular damage because of their cytotoxic effects. However, there should be some cases where the inhibition of NTCP plays a major role in drug-induced cholestasis, considering the importance of the uptake process in the overall transcellular transport of bile acids as described above. Cyclosporin A-induced cholestasis may be one of those. The plasma bile salt concentration was increased in rats after administration of 10 mg/kg cyclosporin A (Stone et al., 1987), indicating that cyclosporin A inhibits the uptake of bile acids from the portal blood into hepato-

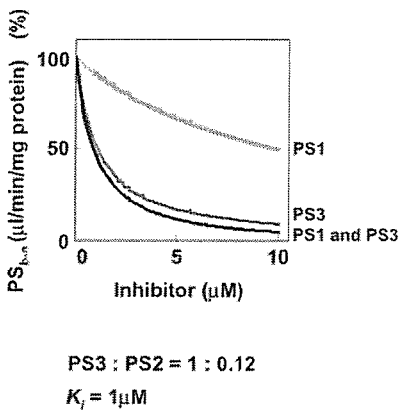

FIG. 5. Simulation of the inhibitory effect of the uptake and/or efflux process on the net basal-to-apical transport of bile taurocholate across hepatocytes. The basal-to-apical clearance $PS_{b\text{-}a}$ of taurocholate across hepatocytes was calculated in the cases where the influx clearance, PS1, the efflux clearance, PS3, or both were affected by the inhibitor under the following conditions. The K_m values of PS1 and PS3 are = 30 μM and 6 μM, respectively, according to the reported K_m values for rat Ntcp and rat Bsep (Schroeder et al., 1998; Hagenbuch et al., 1991; Gerloff et al., 1998; Akita et al., 2001). The unbound concentrations of taurocholate in the basal compartment and the intracellular compartment are smaller than these K_m values (fixed at 1 μM). The inhibition constant K_i for both the influx and efflux clearance is K_i = 1 μM; PS2:PS3 = 1:8.2; $PS_{b\text{-}a} = PS1 \cdot PS3/(PS2 + PS3)$, according to the equation under *Data Analysis*. $PS_{b\text{-}a} = PS1 \cdot PS3/(PS2 + PS3)$. The ratio of PS1:PS2:PS3 is substituted by the measured value (PS1:PS2:PS3 = 1.0:0.7:6.0) in the isolated rat liver perfusion studies cited from Akita et al. (2002).

cytes. Moreover, there was no change in liver histology in the cholestasis caused by cyclosporin A (Kukongviriyapan and Stacey, 1991), suggesting that the cytotoxicity brought about by intracellular bile acids here is not very severe. These facts indicate the importance of the inhibition of NTCP, at least in the case of cyclosporin A-induced cholestasis.

In conclusion, LLC-NTCP/BSEP cells were used for the detection of the inhibitory effect of drugs on NTCP and/or BSEP, although the quantitative evaluation of the inhibitory effect on BSEP appears to be difficult at the present time, compared with transport studies using membrane vesicles. Furthermore, to predict the effect of drugs under physiological conditions, we must consider the drug metabolites, which sometimes significantly inhibit BSEP (Funk et al., 2001). Because there is only a minor quantity of hepatic enzymes involved in drug metabolism in LLC-PK1 cells (Gonzalez and Tarloff, 2004), the inhibitory effects observed in this study are speculated to be those produced by drugs in their unchanged forms. The additional expression of such enzymes and uptake transporters of drugs, such as OATP1B1 and OATP1B3, will provide a more useful tool for quantitative measurement of the inhibitory effect on BSEP.

References

Akita H, Suzuki H, Ito K, Kinoshita S, Sato N, Takikawa H, and Sugiyama Y (2001) Characterization of bile acid transport mediated by multidrug resistance associated protein 2 and bile salt export pump. *Biochim Biophys Acta* **1511:**7–16.

Akita H, Suzuki H, and Sugiyama Y (2002) Sinusoidal efflux of taurocholate correlates with the hepatic expression level of Mrp3. *Biochem Biophys Res Commun* **299:**681–687.

Bohan A and Boyer JL (2002) Mechanisms of hepatic transport of drugs: implications for cholestatic drug reactions. *Semin Liver Dis* **22:**123–136.

Bolder U, Trang NV, Hagey LR, Schteingart CD, Ton-Nu HT, Cerre C, Elferink RP, and Hofmann AF (1999) Sulindac is excreted into bile by a canalicular bile salt pump and undergoes a cholehepatic circulation in rats. *Gastroenterology* **117:**962–971.

Boyer JL, Ng OC, Ananthanarayanan M, Hofmann AF, Schteingart CD, Hagenbuch B, Stieger B, and Meier PJ (1994) Expression and characterization of a functional rat liver Na+ bile acid cotransport system in COS-7 cells. *Am J Physiol* **266:**G382–387.

Byrne JA, Strautnieks SS, Mieli-Vergani G, Higgins CF, Linton KJ, and Thompson RJ (2002) The human bile salt export pump: characterization of substrate specificity and identification of inhibitors. *Gastroenterology* **123:**1649–1658.

Cantz T, Nies AT, Brom M, Hofmann AF, and Keppler D (2000) MRP2, a human conjugate export pump, is present and transports fluo 3 into apical vacuoles of Hep G2 cells. *Am J Physiol* **278:**G522–G531.

Cui Y, Konig J, Buchholz JK, Spring H, Leier I, and Keppler D (1999) Drug resistance and ATP-dependent conjugate transport mediated by the apical multidrug resistance protein, MRP2, permanently expressed in human and canine cells. *Mol Pharmacol* **55:**929–937.

Fattinger K, Cattori V, Hagenbuch B, Meier PJ, and Stieger B (2000) Rifamycin SV and rifampicin exhibit differential inhibition of the hepatic rat organic anion transporting polypeptides, Oatp1 and Oatp2. *Hepatology* **32:**82–86.

Funk C, Ponelle C, Scheuermann G, and Pantze M (2001) Cholestatic potential of troglitazone as a possible factor contributing to troglitazone-induced hepatotoxicity: in vivo and in vitro interaction at the canalicular bile salt export pump (Bsep) in the rat. *Mol Pharmacol* **59:**627–635.

Gerloff T, Stieger B, Hagenbuch B, Madon J, Landmann L, Roth J, Hofmann AF, and Meier PJ (1998) The sister of P-glycoprotein represents the canalicular bile salt export pump of mammalian liver. *J Biol Chem* **273:**10046–10050.

Gonzalez RJ and Tarloff JB (2004) Expression and activities of several drug-metabolizing enzymes in LLC-PK1 cells. *Toxicol In Vitro* **18:**887–894.

Hagenbuch B, Stieger B, Foguet M, Lubbert H, and Meier PJ (1991) Functional expression cloning and characterization of the hepatocyte Na+/bile acid cotransport system. *Proc Natl Acad Sci USA* **88:**10629–10633.

Hayashi H, Takada T, Suzuki H, Akita H, and Sugiyama Y (2005) Two common PFIC2 mutations are associated with the impaired membrane trafficking of BSEP/ABCB11. *Hepatology* **41:**916–924.

Holzinger F, Schteingart CD, Ton-Nu HT, Cerre C, Steinbach JH, Yeh HZ, and Hofmann AF (1998) Transport of fluorescent bile acids by the isolated perfused rat liver: kinetics, sequestration, and mobilization. *Hepatology* **28:**510–520.

Kim RB, Leake B, Cvetkovic M, Roden MM, Nadeau J, Walubo A, and Wilkinson GR (1999) Modulation by drugs of human hepatic sodium-dependent bile acid transporter (sodium taurocholate cotransporting polypeptide) activity. *J Pharmacol Exp Ther* **291:**1204–1209.

Kukongviriyapan V and Stacey NH (1991) Chemical-induced interference with hepatocellular transport. Role in cholestasis. *Chem-Biol Interact* **77:**245–261.

Lowry OH, Rosebrough NJ, Farr AL, and Randall RJ (1951) Protein measurement with the Folin phenol reagent. *J Biol Chem* **193:**265–2751.

Maglova LM, Jackson AM, Meng XJ, Carruth MW, Schteingart CD, Ton-Nu HT, Hofmann AF, and Weinman SA (1995) Transport characteristics of three fluorescent conjugated bile acid analogs in isolated rat hepatocytes and couplets. *Hepatology* **22:**637–647.

Meier PJ, Eckhardt U, Schroeder A, Hagenbuch B, and Stieger B (1997) Substrate specificity of sinusoidal bile acid and organic anion uptake systems in rat and human liver. *Hepatology* **26:**1667–1677.

Meier PJ and Stieger B (2002) Bile salt transporters. *Annu Rev Physiol* **64:**635–661.

Mita S, Suzuki H, Akita H, Hayashi H, Onuki R, Hofmann AF, and Sugiyama Y (2006) Vectorial transport of unconjugated and conjugated bile salts by monolayers of LLC-PK1 cells doubly transfected with human NTCP and BSEP or with rat Ntcp and Bsep. *Am J Physiol* **290:**G550–556.

Mita S, Suzuki H, Akita H, Stieger B, Meier PJ, Hofmann AF, and Sugiyama Y (2005) Vectorial transport of bile salts across MDCK cells expressing both rat Na+-taurocholate cotransporting polypeptide and rat bile salt export pump. *Am J Physiol* **288:**G159–G167.

Mohi-ud-din R and Lewis JH (2004) Drug- and chemical-induced cholestasis. *Clin Liver Dis* **8:**95–132.

Noe J, Stieger B, and Meier PJ (2002) Functional expression of the canalicular bile salt export pump of human liver. *Gastroenterology* **123:**1659–1666.

Schroeder A, Eckhardt U, Stieger B, Tynes R, Schteingart CD, Hofmann AF, Meier PJ, and Hagenbuch B (1998) Substrate specificity of the rat liver Na(+)-bile salt cotransporter in Xenopus laevis oocytes and in CHO cells. *Am J Physiol* **274:**G370–G375.

Sorscher S, Lillienau J, Meinkoth JL, Steinbach JH, Schteingart CD, Feramisco J, and Hofmann AF (1992) Conjugated bile acid uptake by Xenopus laevis oocytes induced by microinjection with ileal Poly A+ mRNA. *Biochem Biophys Res Commun* **186:**1455–1462.

Stieger B, Fattinger K, Madon J, Kullak-Ublick GA, and Meier PJ (2000) Drug- and estrogen-induced cholestasis through inhibition of the hepatocellular bile salt export pump (Bsep) of rat liver. *Gastroenterology* **118:**422–430.

Stone BG, Udani M, Sanghvi A, Warty V, Plocki K, Bedetti CD, and Van Thiel DH (1987) Cyclosporin A-induced cholestasis. The mechanism in a rat model. *Gastroenterology* **93:**344–351.

Strautnieks SS, Bull LN, Knisely AS, Kocoshis SA, Dahl N, Arnell H, Sokal E, Dahan K, Childs S, Ling V, et al. (1998) A gene encoding a liver-specific ABC transporter is mutated in progressive familial intrahepatic cholestasis. *Nat Genet* **20:**233–238.

Trauner M and Boyer JL (2003) Bile salt transporters: molecular characterization, function, and regulation. *Physiol Rev* **83:**633–671.

Wang EJ, Casciano CN, Clement RP, and Johnson WW (2003) Fluorescent substrates of sister-P-glycoprotein (BSEP) evaluated as markers of active transport and inhibition: evidence for contingent unequal binding sites. *Pharm Res (NY)* **20:**537–544.

Wheeler HO (1972) Secretion of bile acids by the liver and their role in the formation of hepatic bile. *Arch Intern Med* **130:**533–541.

Wheeler HO, Ross ED, and Bradley SE (1968) Canalicular bile production in dogs. *Am J Physiol* **214:**866–8748.

Wolkoff AW and Cohen DE (2003) Bile acid regulation of hepatic physiology: I. Hepatocyte transport of bile acids. *Am J Physiol* **284:**G175–G179.

Address correspondence to: Yuichi Sugiyama, Department of Molecular Pharmacokinetics, Graduate School of Pharmaceutical Sciences, The University of Tokyo, 7-3-1 Hongo, Bunkyo-ku, Tokyo 113-0033, Japan. E-mail: sugiyama@mol.f.u-tokyo.ac.jp

0090-9556/06/3407-1247–1254$20.00
DRUG METABOLISM AND DISPOSITION
Copyright © 2006 by The American Society for Pharmacology and Experimental Therapeutics
DMD 34:1247–1254, 2006

Vol. 34, No. 7
8938/3122648
Printed in U.S.A.

INVOLVEMENT OF TRANSPORTERS IN THE HEPATIC UPTAKE AND BILIARY EXCRETION OF VALSARTAN, A SELECTIVE ANTAGONIST OF THE ANGIOTENSIN II AT1-RECEPTOR, IN HUMANS

Wakaba Yamashiro, Kazuya Maeda, Masakazu Hirouchi, Yasuhisa Adachi, Zhuohan Hu, and Yuichi Sugiyama

Graduate School of Pharmaceutical Sciences, the University of Tokyo, Tokyo, Japan (W.Y., K.M., M.H., Y.S.); Daiichi Pure Chemicals Co., Ltd., Tokyo, Japan (Y.A.); and Research Institute for Liver Diseases, Shanghai, China (Z.H.)

Received December 13, 2005; accepted April 18, 2006

ABSTRACT:

Valsartan is a highly selective angiotensin II AT1-receptor antagonist for the treatment of hypertension. Valsartan is mainly excreted into the bile in unchanged form. Because valsartan has an anionic carboxyl group, we hypothesized that a series of organic anion transporters could be involved in its hepatic clearance. In this study, to identify transporters that mediate the hepatic uptake and biliary excretion of valsartan and estimate the contribution of each transporter to the overall hepatic uptake and efflux, we characterized its transport using transporter-expressing systems, human cryopreserved hepatocytes, and Mrp2-deficient Eisai hyperbilirubinemic rats (EHBRs). Valsartan was significantly taken up into organic anion-transporting polypeptide (OATP) 1B1 (OATP2/OATP-C)- and OATP1B3 (OATP8)-expressing HEK293 cells. We also observed saturable uptake into human hepatocytes. Based on our estimation, the relative contribution of OATP1B1 to the uptake of valsartan in human hepatocytes depends on the batch, ranging from 20 to 70%. Regarding efflux transporters, the ratio of basal-to-apical transcellular transport of valsartan to that in the opposite direction in OATP1B1/MRP2 (multidrug resistance-associated protein 2) double transfected cells was the highest among the three kinds of double transfectants, OATP1B1/MRP2, OATP1B1/multidrug resistance 1, and OATP1B1/breast cancer resistance protein-expressing MDCKII cells. We observed saturable ATP-dependent transport into membrane vesicles expressing human MRP2. We also found that the elimination of intravenously administered valsartan from plasma was markedly delayed, and the biliary excretion was severely impaired in EHBR compared with normal Sprague-Dawley rats. These results suggest that OATP1B1 and OATP1B3 as the uptake transporters and MRP2 as the efflux transporter are responsible for the efficient hepatobiliary transport of valsartan.

Valsartan is an antihypertensive drug acting on angiotensin II AT1 receptors. It has been reported that approximately 70% of the total clearance of valsartan is accounted for by hepatic clearance (Flesch et al., 1997). Valsartan undergoes a minor degree of metabolism involving 4-hydroxylation, whereas 85% of orally administered valsartan is excreted into feces in unchanged form (Waldmeier et al., 1997). Considering that the bioavailability is approximately 40% and the hepatic clearance is much less than the hepatic blood flow (Flesch et al., 1997), most of the drug passing into the bile is in the unmetabolized form. From these facts, valsartan is thought to be mainly excreted into the bile in unchanged form. However, the molecular mechanism of the hepatobiliary transport of valsartan has not been elucidated.

When valsartan is given orally to rats, the hepatic concentration is about 7 to 10 times higher than the plasma concentration, suggesting that valsartan is selectively distributed to the liver (interview form of Diovan tablet). Because valsartan is a hydrophilic compound with a log D value (pH = 7.0) of −0.34 and it has an anionic carboxyl group, it should have difficulty in crossing the plasma membrane. Therefore, a number of organic anion transporters could be involved in the hepatic transport of valsartan.

The organic anion-transporting polypeptide (OATP) family transporters play an important role in the transport of organic anions (Hagenbuch and Meier, 2004). Among them, OATP1B1 (OATP-C/OATP2) and OATP1B3 (OATP8) are thought to be responsible for the hepatic uptake of several organic anions in humans because of their selective expression in liver and broad substrate specificities (Hagenbuch and Meier, 2004). They can also accept a variety of clinically used drugs, such as 3-hydroxy-3-methylglutaryl CoA reductase inhibitors, rifampin, and methotrexate (Hsiang et al., 1999; Abe

This work was partly supported by Health and Labor Sciences Research Grants from the Ministry of Health, Labor, and Welfare for the Research on Advanced Medical Technology and by Grant-in Aid for Young Scientists B (17790113) from the Ministry of Education, Culture, Sports, Science, and Technology.

Article, publication date, and citation information can be found at http://dmd.aspetjournals.org.

doi:10.1124/dmd.105.008938.

ABBREVIATIONS: OATP, organic anion-transporting polypeptide; AUC, area under the plasma concentration-time curve; BCRP, breast cancer resistance protein; CCK-8, cholecystokinin octapeptide; E_1S, estrone-3-sulfate; $E_2 17\beta G$, estradiol-17β-glucuronide; EHBR, Eisai hyperbilirubinemic rat; MRP2, multidrug resistance-associated protein 2; MDR1, multidrug resistance 1; *PS*, permeability surface; SD, Sprague-Dawley; CL, clearance.

et al., 2001; Nakai et al., 2001; Vavricka et al., 2002; Shitara et al., 2003a; Hirano et al., 2004). OATP2B1 (OATP-B) is also expressed in the basolateral membrane of human liver. Its substrate specificity is relatively narrow compared with OATP1B1 and 1B3, but some of the OATP1B1 and OATP1B3 substrates can also be recognized by OATP2B1 (Tamai et al., 2000; Kullak-Ublick et al., 2001). Conversely, multidrug resistance 1 (MDR1), multidrug resistance-associated protein 2 (MRP2), and breast cancer resistance protein (BCRP) can be involved in the hepatic efflux transport of organic anions (Chandra and Brouwer, 2004).

In general, the substrate specificity of each transporter is very broad and it is often very similar to that of other transporters, suggesting that a substrate can be recognized by multiple transporters. Now we can use human cryopreserved hepatocytes for the evaluation of transporter-mediated uptake. Shitara et al. (2003a) have succeeded in clarifying the importance of OATP1B1-mediated inhibition in the clinical drug-drug interaction between cerivastatin and cyclosporin A from in vitro experiments using human cryopreserved hepatocytes and transporter expression systems.

Hirano et al. (2004) have recently published their methodology for estimating the quantitative contribution of OATP1B1 and OATP1B3 to the hepatic uptake of compounds. In one of their approaches, they calculated the ratio of the uptake clearance of transporter-selective substrates in human cryopreserved hepatocytes to that in transporter-expression systems, and then estimated the hepatic uptake of test compounds mediated by certain transporters by multiplying that ratio by the clearance of the test compounds in transporter-expressing cells. We applied this method to the calculation of the contribution of OATP1B1 and OATP1B3 to the human hepatic uptake. To check the involvement of efflux transporters in the biliary excretion of compounds, Matsushima et al. (2005) have shown that OATP1B1/MDR1, OATP1B1/MRP2, and OATP1B1/BCRP double transfectants can be used for the rapid identification of anionic bisubstrates of OATP1B1 and each efflux transporter by measuring the vectorial transport of substrates across each monolayer. If valsartan is a substrate of OATP1B1, these cell lines should help us to identify which transporters are involved in its biliary excretion in humans.

In this study, we analyzed the involvement and relative contribution of OATP1B1 and OATP1B3 to the hepatic uptake of valsartan using human cryopreserved hepatocytes and transporter-expressing cells and identified the transporters responsible for the biliary excretion of valsartan using double transfectants and transporter-expressing vesicles. We also checked the involvement of MRP2 in the pharmacokinetics of valsartan in vivo using Eisai hyperbilirubinemic rats (EHBR), in which Mrp2 is deficient.

Materials and Methods

Materials. [^{3}H]Valsartan (80.9 Ci/mmol) and unlabeled valsartan were kindly donated by Novartis Pharma K.K. (Basel, Switzerland). [^{3}H]Estradiol-17β-glucuronide ($E_2$17βG) (45 Ci/mmol) and [^{3}H]estrone-3-sulfate (46 Ci/mmol) were purchased from PerkinElmer Life and Analytical Sciences (Boston, MA), and [^{3}H]cholecystokinin octapeptide (CCK-8) (77 Ci/mmol) was purchased from GE Healthcare Bio-Sciences (Buckinghamshire, UK). Unlabeled $E_2$17βG, estrone-3-sulfate, and CCK-8 were purchased from Sigma-Aldrich (St. Louis, MO). All other chemicals were of analytical grade and commercially available.

Cell Culture. Transporter-expressing or vector-transfected HEK293 cells and MDCKII cells were grown in Dulbecco's modified Eagle's medium low glucose (Invitrogen, Carlsbad, CA) supplemented with 10% fetal bovine serum (Sigma, St. Louis, MO), 100 U/ml penicillin, 100 μg/ml streptomycin, and 0.25 μg/ml amphotericin B at 37°C with 5% CO_2 and 95% humidity. LLC-PK1 cells were cultured in Medium 199 (Invitrogen) supplemented with 10% fetal bovine serum (Sigma), 100 U/ml penicillin, and 100 μg/ml streptomycin.

Transport Study Using Transporter Expression Systems. Cells were seeded in 12-well plates coated with poly-L-lysine/poly-L-ornithine at a density of 1.5×10^5 cells/well 72 h before transport assay. For the transport study, the cell culture medium was replaced with culture medium supplemented with 5 mM sodium butyrate 24 h before transport assay to induce the expression of OATP1B1, OATP1B3, or OATP2B1.

The transport study was carried out as described previously (Hirano et al., 2004, 2006). Uptake was initiated by adding Krebs-Henseleit buffer containing radiolabeled and unlabeled substrates after cells had been washed twice and preincubated with Krebs-Henseleit buffer at 37°C for 15 min. The Krebs-Henseleit buffer consisted of 118 mM NaCl, 23.8 mM $NaHCO_3$, 4.8 mM KCl, 1.0 mM KH_2PO_4, 1.2 mM $MgSO_4$, 12.5 mM HEPES, 5.0 mM glucose, and 1.5 mM $CaCl_2$ adjusted to pH 7.4. The uptake was terminated at designated times by adding ice-cold Krebs-Henseleit buffer after removal of the incubation buffer. Then, cells were washed twice with 1 ml of ice-cold Krebs-Henseleit buffer, solubilized in 500 μl of 0.2 N NaOH, and kept overnight at 4°C. Aliquots (500 μl) were transferred to scintillation vials after adding 250 μl of 0.4 N HCl. The radioactivity associated with the cells and incubation buffer was measured in a liquid scintillation counter (LS6000SE; Beckman Coulter, Inc., Fullerton, CA) after adding 2 ml of scintillation fluid (Clear-sol I; Nacalai Tesque, Kyoto, Japan) to the scintillation vials. The remaining 50 μl of cell lysate was used to determine the protein concentration by the method of Lowry et al. (1951) with bovine serum albumin as a standard.

Transport Study Using Human Cryopreserved Hepatocytes. This experiment was performed as described previously (Hirano et al., 2004). Cryopreserved human hepatocytes were purchased from In Vitro Technologies (Baltimore, MD) (lot 094 and OCF) and from the Research Institute for Liver Disease (Shanghai, China) (lot 03-013). Immediately before the study, the hepatocytes (1-ml suspension) were thawed at 37°C, then quickly suspended in 10 ml of ice-cold Krebs-Henseleit buffer and centrifuged (50g) for 2 min at 4°C, followed by removal of the supernatant. This procedure was repeated once more to remove cryopreservation buffer, and then the cells were resuspended in the same buffer to give a cell density of 1.0×10^6 viable cells/ml for the uptake study. The number of viable cells was determined by trypan blue staining. Before the uptake studies, the cell suspensions were prewarmed in an incubator at 37°C for 3 min. The uptake studies were initiated by adding an equal volume of buffer containing labeled and unlabeled substrates to the cell suspension. After incubation at 37°C for 0.5, 2, or 5 min, the reaction was terminated by separating the cells from the substrate solution. For this purpose, an aliquot of 80-μl incubation mixture was collected and placed in a centrifuge tube (450 μl) containing 50 μl of 2 N NaOH under a layer of 100 μl of oil (density, 1.015; a mixture of silicone oil and mineral oil; Sigma-Aldrich), and subsequently, the sample tube was centrifuged for 10 s using a tabletop centrifuge (10,000g; Beckman Microfuge E; Beckman Coulter, Inc.). During this process, hepatocytes passed through the oil layer into the alkaline solution. After an overnight incubation in alkali to dissolve the hepatocytes, the centrifuge tube was cut and each compartment was transferred to a scintillation vial. The compartment containing the dissolved cells was neutralized with 50 μl of 2 N HCl and mixed with scintillation cocktail, and the radioactivity was measured in a liquid scintillation counter.

Transcellular Transport Study Using Double Transfected Cells. The protocol has been described in detail previously (Matsushima et al., 2005). In brief, transfected MDCKII cells were seeded in a Transwell membrane insert (6.5-mm diameter, 0.4-μm pore size; Corning Costar, Cambridge, MA) at a density of 1.4×10^5 cells per well 96 h before the transport study. Among a series of cell lines we used in this experiment, human MDR1, MRP2, and OATP1B1 were stably transfected into MDCKII cells as shown previously (Evers et al., 1998; Matsushima et al., 2005). Human BCRP cDNA was transduced into MDCKII cells by the infection of recombinant adenovirus 48 h before the transport study. The cell culture medium was replaced with culture medium supplemented with 5 mM sodium butyrate 24 h before the transport assay. For uptake studies, cells were washed three times and preincubated with Krebs-Henseleit buffer. The experiment was initiated by replacing the medium at either the apical or the basal side of the cell layer with complete medium containing ^{3}H-labeled and unlabeled valsartan or $E_2$17βG (0.1 μM). The cells were incubated at 37°C and aliquots of medium were taken from each compartment at several time points. Radioactivity in 100 μl of medium was measured in a liquid scintillation counter after addition of 2 ml of scintillation

fluid. At the end of the experiments, the cells were washed three times with 1.5 ml of ice-cold Krebs-Henseleit buffer and solubilized in 500 μl of 0.2 N NaOH. After addition of 100 μl of 1 N HCl, 400-μl aliquots were transferred to scintillation vials. Then, 50-μl aliquots of cell lysate were used to determine protein concentrations by the method of Lowry et al. (1951) with bovine serum albumin as a standard.

Vesicle Transport Assay. The preparation procedure of the membrane vesicles expressing human MRP2 was described previously (Hirouchi et al., 2004). The transport medium (10 mM Tris, 250 mM sucrose, and 10 mM $MgCl_2$, pH 7.4) contained the labeled and unlabeled valsartan, 5 mM ATP, and an ATP-regenerating system (10 mM creatine phosphate and 100 μg/μl creatine phosphokinase). An aliquot of transport medium (15 μl) was mixed rapidly with the vesicle suspension (5 μg of protein in 5 μl). The transport reaction was stopped by the addition of 1 ml of ice-cold buffer containing 250 mM sucrose, 0.1 M NaCl, and 10 mM Tris-HCl buffer (pH 7.4). The stopped reaction mixture was passed through a 0.45-μm HA filter (Millipore Corp., Billerica, MA) and then washed twice with 5 ml of stop solution. The radioactivity retained on the filter was measured in a liquid scintillation counter after the addition of scintillation cocktail. Ligand uptake was normalized in terms of the amount of membrane protein.

In Vivo Pharmacokinetic Study. Male Sprague-Dawley (SD) rats and EHBRs (7–8 weeks old) were purchased from Nippon SLC (Shizuoka, Japan). All animals were maintained under standard conditions with a reverse dark-light cycle and were treated humanely. Food and water were available ad libitum. This study was carried out in accordance with the guidelines provided by the Institutional Animal Care Committee (Graduate School of Pharmaceutical Sciences, The University of Tokyo, Tokyo, Japan). SD rats and EHBRs were anesthetized by inhalation of diethyl ether. The abdomen was opened with a midline incision and the common bile duct was cannulated with a polyethylene tube (Becton Dickinson Primary Care Diagnostics, Sparks, MD). The phosphate-buffered saline containing [^{3}H]valsartan (8 μCi/ml) and unlabeled valsartan (1 mg/ml) was injected into a femoral vein (1 ml/kg body weight). Blood samples were collected from a femoral artery and bile samples were collected in preweighed tubes at designated times. The total radioactivity in plasma and bile samples was measured in a liquid scintillation counter.

Kinetic Analyses of Uptake Transporters. Ligand uptake was expressed as the uptake volume [μl/mg protein], given as the amount of radioactivity associated with the cells [dpm/mg protein] divided by its concentration in the incubation medium [dpm/μl]. Specific uptake was obtained by subtracting the uptake into vector-transfected cells from the uptake into cDNA-transfected cells. Kinetic parameters were obtained using the following equation:

$$v = \frac{V_{max} \cdot S}{K_m + S} + P_{dif} \cdot S \quad (1)$$

where v is the uptake velocity of the substrate (pmol/min/mg protein), S is the substrate concentration in the medium (μM), K_m is the Michaelis constant (μM), V_{max} is the maximum uptake rate (pmol/min/mg protein), and P_{dif} is the nonsaturable uptake clearance (μl/min/mg protein). Fitting was performed by the nonlinear least-squares method using a MULTI program (Yamaoka et al., 1981), and the Damping Gauss-Newton Method algorithm was used for curve fitting. The input data were weighted as the reciprocal of the observed values.

To determine the saturable hepatic uptake clearance in human hepatocytes, we first determined the hepatic uptake clearance ($CL_{(2\ min\text{-}0.5\ min)}$) ($\mu$l/min/$10^6$ cells) by calculating the slope of the uptake volume (V_d) (μl/10^6 cells) between 0.5 and 2 min (eq. 2). The saturable component of the hepatic uptake clearance (CL_{hep}) was determined by subtracting $CL_{(2\ min\text{-}0.5\ min)}$ in the presence of 100 μM substrate (excess) from that in the presence of 1 μM substrate (tracer quantity) (eq. 3).

$$CL_{(2\ min-0.5\ min)} = \frac{V_{d,2\ min} - V_{d,0.5\ min}}{2 - 0.5} \quad (2)$$

$$CL_{hep} = CL_{(2\ min-0.5\ min),tracer} - CL_{(2\ min-0.5\ min),excess} \quad (3)$$

where $CL_{(2\ min\text{-}0.5\ min),\ tracer}$ and $CL_{(2\ min\text{-}0.5\ min),\ excess}$ represent the $CL_{(2\ min\text{-}0.5\ min)}$ values estimated in the presence of 1 and 100 μM substrate, respectively.

Estimation of the Relative Contribution of Each Transporter to the Hepatic Uptake. This method for estimating the contribution of OATP1B1 and OATP1B3 to the overall hepatic uptake has been used previously (Hirano et al., 2004). In this analysis, estrone-3-sulfate and CCK-8 were chosen as transporter-selective substrates of OATP1B1 and OATP1B3, respectively. The ratio of the uptake clearance of the reference compounds in human hepatocytes to that in the expression system was calculated and defined as $R_{act,\ OATP1B1}$ and $R_{act,\ OATP1B3}$. The uptake clearance mediated by OATP1B1 and OATP1B3 in human hepatocytes was separately calculated by multiplying the uptake clearance of valsartan in transporter-expressing cells ($CL_{OATP1B1,\ test}$ and $CL_{OATP1B3,\ test}$) by $R_{act,\ OATP1B1}$ and $R_{act,\ OATP1B3}$, respectively, as described in the following equations:

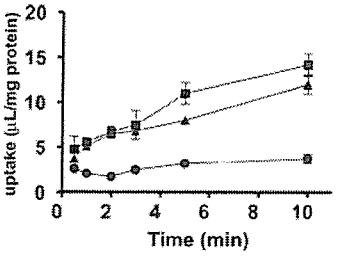

FIG. 1. Time profiles of the uptake of valsartan by OATP1B1- and OATP1B3-expressing HEK293 cells. Squares, triangles, and circles represent the uptake in OATP1B1- and OATP1B3-expressing cells and vector-control cells, respectively. Each point represents the mean ± S.E. (n = 3).

$$R_{act,OATP1B1} = \frac{CL_{Hep,E_1S}}{CL_{OATP1B1,E_1S}} \quad (4)$$

$$R_{act,OATP1B3} = \frac{CL_{Hep,CCK\text{-}8}}{CL_{OATP1B3,CCK\text{-}8}} \quad (5)$$

$$CL_{hep,test,OATP1B1} = CL_{OATP1B1,test} \cdot R_{act,OATP1B1} \quad (6)$$

$$CL_{hep,test,OATP1B3} = CL_{OATP1B3,test} \cdot R_{act,OATP1B3} \quad (7)$$

Kinetic Analyses of Efflux Transporters. The basal-to-apical transcellular clearance (CL_{trans}) was calculated by dividing the steady-state efflux velocity for the transcellular transport (V_{apical}) by the ligand concentration in the incubation buffer on the basal side, whereas the efflux clearance across the apical membrane (PS_{apical}) in double transfected cells was obtained by dividing V_{apical} by the intracellular concentration of ligand at 120 min. In the vesicle transport assay, ATP-dependent transporter-specific uptake was calculated by subtracting the uptake in the presence of AMP from that in the presence of ATP. The saturation kinetics of CL_{trans}, PS_{apical}, and ATP-dependent uptake into vesicles were calculated using eq. 1 by the curve-fitting procedure described above.

Pharmacokinetic Analysis. The plasma concentration-time profile was fitted to a biexponential equation and the $AUC_{0-\infty}$ was estimated by integration up to infinity. The initial distribution volume (V_1) was calculated by dividing the dose by the initial plasma concentration estimated from the fitted biexponential equation. The plasma clearance (CL_p) was calculated as Dose/$AUC_{0-\infty}$. The biliary clearance (CL_{bile}) was calculated as the ratio of the cumulative excreted amount in bile over 120 min to the AUC over 120 min ($AUC_{0-120\ min}$).

Results

Uptake of Valsartan by OATP Transporter-Expressing Cells. Valsartan was significantly taken up into OATP1B1- and OATP1B3-expressing HEK293 cells compared with vector-transfected cells in a time-dependent manner (Fig. 1). The saturation kinetics of valsartan by OATP1B1- and OATP1B3-expressing cells and vector-transfected HEK293 was evaluated by the uptake for 5 min, over which time the uptake of valsartan remained linear, and shown as Eadie-Hofstee plots (Fig. 2). The concentration dependence of the uptake of valsartan could be explained by a one-saturable and one-nonsaturable component. Their kinetic parameters are summarized in Table 1. In contrast,

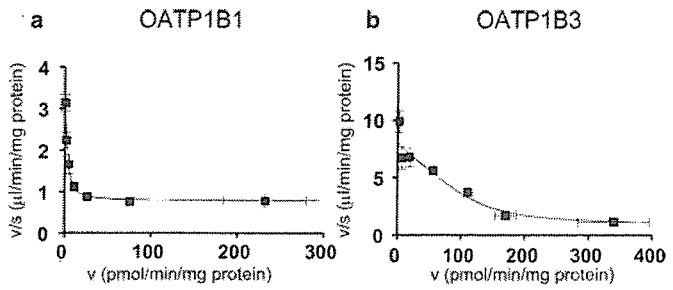

FIG. 2. Eadie-Hofstee plots of the uptake of valsartan by OATP1B1- and OATP1B3-expressing HEK293 cells. The concentration dependence of OATP1B1 (a)- and OATP1B3 (b)-mediated uptake of valsartan is shown as Eadie-Hofstee plots. The uptake of valsartan for 5 min was determined at various concentrations (0.1–300 μM). Each point represents the mean ± S.E. (n = 3).

TABLE 1

Kinetic parameters of the uptake of valsartan by OATP1B1- and OATP1B3-expressing HEK293 cells

Data shown in Fig. 2 were used to determine these parameters calculated by nonlinear regression analysis as described under *Materials and Methods*. Each parameter represents the mean ± computer-calculated S.D.

	K_m	V_{max}	P_{dif}
	μM	*pmol/min/mg protein*	*ml/min/mg protein*
OATP1B1	1.39 ± 0.24	3.85 ± 0.46	0.747 ± 0.022
OATP1B3	18.2 ± 5.9	135 ± 40	0.680 ± 0.223

valsartan was not significantly transported in OATP2B1-expressing HEK293 cells [0.627 ± 0.092 μl/min/mg protein (OATP2B1-expressing HEK293 cells) versus 0.552 ± 0.081 μl/min/mg protein (vector-control cells); mean ± S.E.].

Uptake of Estrone-3-Sulfate, CCK-8, and Valsartan by Human Cryopreserved Hepatocytes. Typical time profiles of the uptake of estrone-3-sulfate, CCK-8, and valsartan in one batch of human hepatocytes (lot OCF) are shown in Fig. 3. The uptake of labeled valsartan by human hepatocytes was inhibited by unlabeled 100 μM valsartan in a concentration-dependent manner (Fig. 4). Time-dependent uptake of all ligands was observed at 1 μM, and this was reduced in the presence of 100 μM unlabeled ligands in all batches of hepatocytes examined in the present study (data not shown). The uptake clearance of these substrates in each batch is listed in Table 2. Based on the data in Table 2, following the method for estimating the contribution of OATP1B1 and OATP1B3 to the overall hepatic uptake described previously (Hirano et al., 2004), we calculated the estimated clearance of valsartan mediated by OATP1B1 and OATP1B3 and the quantitative contribution of these transporters to the hepatic uptake in three batches of human hepatocytes. Our estimation indicated that the relative contribution of OATP1B1 and OATP1B3 depends on the batch of human hepatocytes, ranging from 20% to 70% (as the contribution of OATP1B1) (Table 3).

Transcellular Transport of Valsartan across MDCKII Monolayers. To identify the efflux transporters involved in the biliary excretion of valsartan, we investigated the transcellular transport of valsartan across the MDCKII monolayers expressing uptake and efflux transporters. We could not see any significant vectorial transcellular transport of valsartan in single transfected MDCKII cells expressing OATP1B1, MDR1, MRP2, and BCRP, and vector-transfected control cells. In contrast, as shown in Fig. 5, the basal-to-apical transcellular transport of valsartan in OATP1B1/MRP2 double transfected cells was the largest among three kinds of double transfectants, OATP1B1/MRP2, OATP1B1/MDR1, and OATP1B1/BCRP. In parallel, we also checked the transcellular transport of $E_2$17βG, whose basal-to-apical transport was reported to be observed in three kinds of

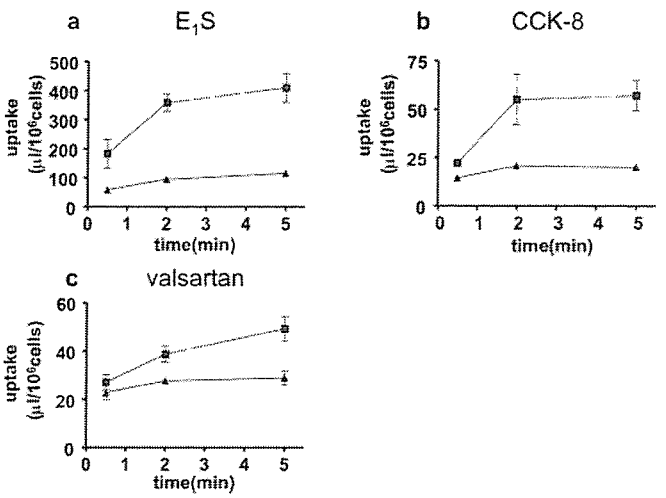

FIG. 3. Typical time profiles of the uptake of estrone-3-sulfate, CCK-8, and valsartan by human hepatocytes (lot OCF). The uptake of estrone-3-sulfate (a), CCK-8 (b), and valsartan (c) for 0.5, 2, and 5 min was determined at two concentrations (squares, 1 μM; triangles, 100 μM) at 37°C. Each point represents the mean ± S.E. (n = 3).

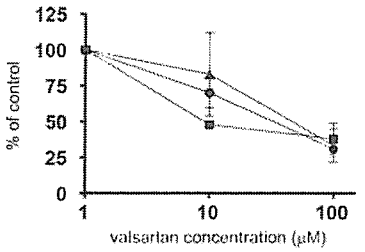

FIG. 4. Concentration dependence of uptake of valsartan by human hepatocytes. The uptake of valsartan for 0.5 and 2 min was determined at three concentrations (1, 10, and 100 μM) at 37°C. The uptake clearance was obtained by subtracting the uptake at 0.5 min from that at 2 min, and the uptake clearance at 1 μM valsartan is defined as 100%. Circles, squares, and triangles represent the uptake in lots OCF, 03-013, and 094, respectively. Each point represents the mean ± S.E. (n = 3).

TABLE 2

Uptake clearance of reference compounds (E_1S and CCK-8) and valsartan in expression systems and human hepatocytes

	Transporter-Expressing Cells		Human Hepatocytes		
	$CL_{OATP1B1}$	$CL_{OATP1B3}$	OCF	094	03-013
	μl/min/mg protein		*μl/min/10^6 cells*		
E_1S	84.6		93.0	98.7	45.2
CCK-8		10.3	17.7	71.6	3.65
valsartan	1.56	0.96	3.55	17.1	6.15

double transfectants we tested (Fig. 5, a–c). The basal-to-apical transport of $E_2$17βG was 36, 8.9, and 6.1 times larger than that in the opposite direction in OATP1B1/MRP2, OATP1B1/MDR1, and OATP1B1/BCRP double transfectants, respectively, which is almost comparable to the previous results (Matsushima et al., 2005). Then, we studied the concentration dependence of the transcellular transport of valsartan in OATP1B1/MRP2-expressing cells (Fig. 6a), and the efflux clearance across the apical membrane (PS_{apical}) was determined by measuring the cellular accumulation of valsartan at 120 min (Fig. 6b). The K_m value of transcellular transport of valsartan (27.5 μM) was smaller than that for PS_{apical} (99.0 μM) (Table. 4).

ATP-Dependent Uptake of Valsartan in Human MRP2-Expressing Membrane Vesicles. To confirm that valsartan is a substrate of human MRP2, the time-dependent uptake of [^{3}H]valsartan by

TABLE 3

Contribution of OATP1B1 and OATP1B3 to the hepatic uptake of valsartan in each batch of human hepatocytes

In the column 'Estimated Clearance of Valsartan,' the lower row shows the percentage of OATP1B1- or OATP1B3-mediated uptake clearance relative to the sum of the estimated clearance mediated by OATP1B1 and OATP1B3. The details of this estimation are described under *Materials and Methods*.

Lot	Ratio of Uptake Clearance $CL_{hep}/CL_{transporter}$		Estimated Clearance of Valsartan	
	$R_{act,OATP1B1}$	$R_{act,OATP1B3}$	OATP1B1	OATP1B3
			μl/min/10⁶ cells	
OCF	1.10	1.72	1.72	1.65
			51.0%	49.0%
094	1.17	6.95	1.83	6.67
			21.5%	78.5%
03–013	0.53	0.35	0.827	0.336
			71.1%	28.9%

TABLE 4

Kinetic parameters of the transcellular transport of valsartan in OATP1B1/MRP2 double transfectant

Data shown in Fig. 6 were used to determine these parameters calculated by nonlinear regression analysis as described under *Materials and Methods*. Each parameter represents the mean ± computer-calculated S.D.

	K_m	V_{max}	P_{dif}
	μM	*pmol/min/mg protein*	*ml/min/mg protein*
Transcellular transport	27.5 ± 4.1	164 ± 24	0.937 ± 0.123
PS_{apical}	99.0 ± 51.1	461 ± 275	0.120 ± 0.610

membrane vesicles prepared from MRP2-expressing LLC-PK1 cells was examined. [^{3}H]Valsartan was significantly taken up into the membrane vesicles expressing MRP2 in an ATP-dependent manner (Fig. 7a), and this uptake could be saturated with K_m, V_{max}, and P_{dif} values of 30.4 ± 17.7 μM, 895 ± 578 pmol/min/mg protein, and 8.88 ± 3.05 μl/min/mg protein, respectively.

Pharmacokinetics of Valsartan in SD Rats and EHBRs. After i.v. administration of 1 mg of valsartan per kg of body weight, we compared the plasma concentration and the biliary excretion of valsartan in SD rats and EHBRs. The plasma concentration was significantly higher in EHBRs compared with SD rats (Fig. 8a). After 2 h, 70% of the total radioactivity injected was excreted into bile in SD rats, whereas in EHBRs, only 15% was excreted (Fig. 8b). The pharmacokinetic parameters of valsartan after i.v. administration in SD rats and EHBRs are summarized in Table. 5. The plasma $AUC_{0-\infty}$ of EHBRs was 17 times higher than that of SD rats, and the total body plasma clearance and biliary clearance were markedly decreased in EHBRs to 6% and 2% of control SD rats, respectively.

Discussion

In humans, valsartan is mainly excreted into bile, mostly in the unchanged form without any significant metabolism (Waldmeier et al., 1997). Considering this physicochemical property, we hypothesized that a series of transporters of organic anions could be involved in the hepatic transport of valsartan. Therefore, in this study, we identified transporters that mediate the hepatic uptake and biliary excretion of valsartan in humans.

First, we performed uptake experiments using OATP1B1 and OATP1B3 expression systems. These transporters are thought to be important for the transport of organic anions in human liver because they are selectively expressed in the liver and can accept a wide variety of compounds. We found that valsartan can be taken up via both OATP1B1 and OATP1B3. In contrast, no significant uptake of valsartan was observed in OATP2B1-expressing cells compared with vector-transfected control cells, suggesting that the contribution of

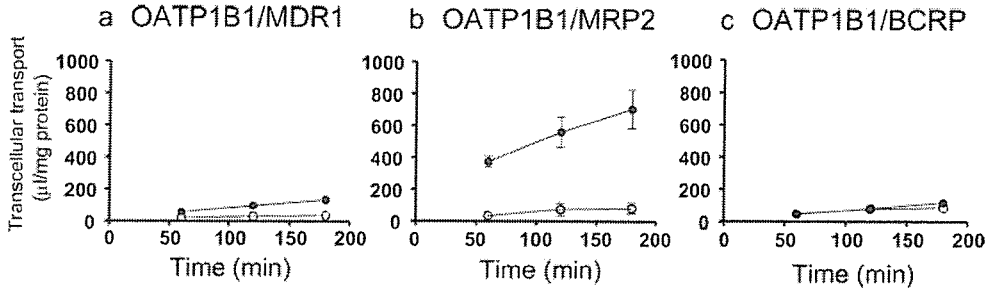

FIG. 5. Time profiles of the transcellular transport of valsartan across MDCKII monolayers expressing transporters. Transcellular transport of valsartan (0.1 μM) across MDCKII monolayers expressing OATP1B1/MDR1 (a), OATP1B1/MRP2 (b), and OATP1B1/BCRP (c) was observed. Open circles and closed circles represent the transcellular transport in the apical-to-basal and basal-to-apical directions, respectively. Each point represents the mean ± S.E. (n = 3).

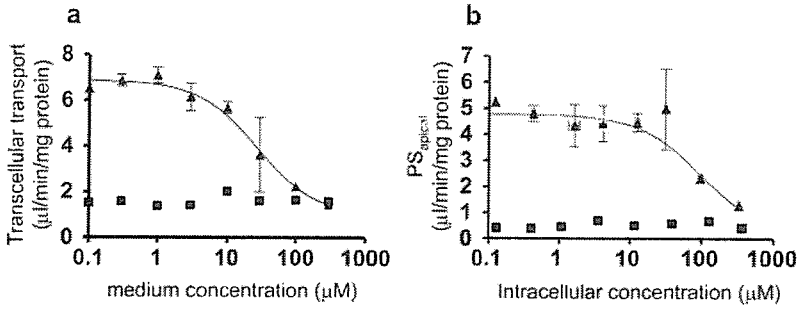

FIG. 6. Concentration dependence of the transcellular clearance (a) and intrinsic clearance across the apical membrane (b) in OATP1B1/MRP2-expressing MDCKII cells. The transcellular transport of valsartan across OATP1B1/MRP2 MDCKII monolayer was observed for 2 h at 37°C (a). The intrinsic clearance for the transport of valsartan across the apical membrane (PS_{apical}) was determined by dividing the transcellular transport velocity of valsartan determined over 2 h by the cellular concentration determined at the end of the experiments (2 h) (b). Triangles and squares represent the transcellular transport across OATP1B1/MRP2 double transfectants and vector-transfected control cells, respectively. Each point represents the mean ± S.E. (n = 3).

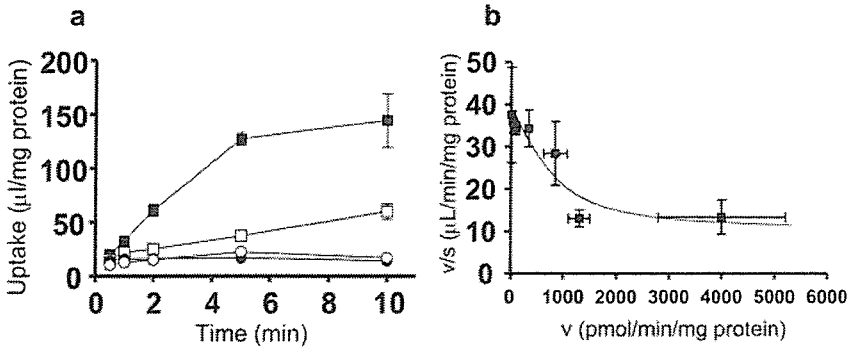

FIG. 7. The ATP-dependent transport of valsartan in MRP2-expressing LLC-PK1 cells. Time profiles for the uptake of valsartan were measured in isolated membrane vesicles prepared from LLC-PK1 cells expressing MRP2 (a). Membrane vesicles were incubated at 37°C with valsartan (0.1 μM) in the medium in the presence of ATP (closed symbols) or AMP (open symbols) for designated periods (0.5, 1, 2, 5, or 10 min). Squares and circles represent the uptake of membrane vesicles expressing MRP2 and control vesicles infected only with adenovirus containing tetracycline-responsive transcriptional activator, respectively. The concentration dependence of MRP2-mediated uptake of valsartan is shown as Eadie-Hofstee plots (b). The uptake of valsartan for 2 min was determined at various concentrations (0.3–300 μM). Each point represents the mean ± S.E. (n = 3).

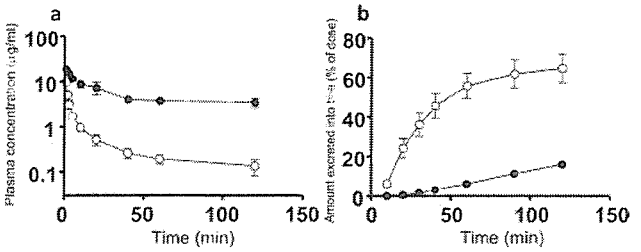

FIG. 8. Biliary elimination of valsartan in male SD rats and EHBRs. Rats were injected with valsartan (1 mg/kg body weight dissolved in phosphate-buffered saline) into a femoral vein after cannulation of the bile duct. The time profiles of the plasma concentration (a) and cumulative biliary excretion (b) of valsartan in SD rats (open circles) and EHBRs (closed circles) are shown. Each point represents the mean ± S.E. (n = 3).

OATP2B1 is negligible as far as hepatic uptake is concerned. To understand the relative importance of OATP1B1 and OATP1B3 in the hepatic uptake of valsartan, we cannot easily compare the uptake clearance of OATP1B1 and OATP1B3 in transporter expression systems because the relative expression level of OATP1B1 and OATP1B3 is different in human hepatocytes and expression systems. To overcome this problem, Hirano et al. (2004) established a methodology for estimating the contribution of OATP1B1 and OATP1B3 to the hepatic uptake of compounds. We used the approach called the relative activity factor (RAF) method (Hirano et al., 2004), in which we use transporter-specific ligands (estrone-3-sulfate for OATP1B1, CCK-8 for OATP1B3). To determine the contribution of transporters, we used three different batches of human hepatocytes prepared from independent donors because Shitara et al. (2003b) reported that there were large interbatch differences in uptake activity in human cryopreserved hepatocytes. Valsartan was taken up by all batches of human hepatocytes in a saturable manner. In the presence of 100 μM valsartan, the time course of the uptake of valsartan was almost flat for 5 min, whereas the uptake of 1 μM valsartan was clearly observed by 2 min, indicating that 100 μM valsartan is enough to saturate the transporter-mediated uptake. This is consistent with our results showing that the K_m values of OATP1B1 and OATP1B3 were much lower than 100 μM. We observed the self-saturation of the uptake of valsartan in human hepatocytes at three concentrations (1, 10, and 100 μM), and the uptake clearance at 10 μM was decreased to half of that at 1 μM (Fig. 4).

According to the manufacturer's interview form, the maximum plasma concentration (C_{max}) and AUC are directly proportional to the dose in Japanese healthy male subjects. After oral administration of 160 mg of valsartan, the C_{max} is 12 μM and the plasma unbound fraction is 5 to 7% (Colussi et al., 1997), indicating that the unbound plasma concentration of valsartan is 0.60 to 0.84 μM. This value is lower than the K_m values obtained from OATP-expressing systems and human hepatocytes. This is consistent with the fact that valsartan exhibits linear pharmacokinetics over the clinical dose range. The absolute value of the uptake clearance of reference compounds in each batch of hepatocytes was different from the reported values (Hirano et al., 2004). We have sometimes experienced that the viability of the hepatocytes and the uptake clearance of compounds are different between the individual tubes even when they are prepared from the same human liver. To overcome this problem, we always check the uptake clearance of reference compounds such as $E_2$17βG in parallel with the test compounds and the relative values of the uptake clearance of reference compounds and test compounds can be discussed.

Regarding the contribution of OATP1B1 and OATP1B3 to the hepatic uptake of valsartan, our results indicate that both OATP1B1 and OATP1B3 are involved in the uptake of valsartan in human hepatocytes, although the estimated contribution of each batch of hepatocytes was different (Table. 3). Previous reports suggest that pitavastatin, a novel 3-hydroxy-3-methylglutaryl CoA reductase inhibitor, and estradiol-17β-glucuronide, a typical substrate of both OATP1B1 and OATP1B3, are taken up into hepatocytes predominantly via OATP1B1 (Hirano et al., 2004), whereas the hepatic uptake of fexofenadine, an H_2-receptor antagonist, is thought to be mainly via OATP1B3 rather than OATP1B1 (Shimizu et al., 2005). Therefore, although OATP1B1 is generally believed to be responsible for the hepatic uptake of several kinds of drugs, we think that the relative importance of OATP1B1 and OATP1B3 depends on the drugs themselves, and this estimation method is useful for predicting their contribution to hepatic clearance. Very recently, we found that telmisartan is recognized exclusively by OATP1B3, and not OATP1B1 (Ishiguro et al., 2006). So, even within the same category of drugs, the relative contribution of OATP1B1 and OATP1B3 is different. This might result in differences in the pharmacokinetics and subsequent pharmacological effects when the function of certain transporters is changed by a variety of conditions, such as genetic polymorphism (e.g., OATP1B1*15) (Nishizato et al., 2003). Therefore, we think that it is important to evaluate the contribution of each transporter to the hepatic elimination of drugs because we can then estimate the change in the overall hepatic clearance quantitatively when the expression level and/or transport function of certain transporters is changed by pathophysiological conditions, single-nucleotide polymorphisms, and

TABLE 5

Summary for the pharmacokinetic parameters of valsartan in SD rats and EHBRs

Pharmacokinetic parameters are expressed as mean ± S.E. (n = 3).

	$AUC_{0-\infty}$	V_1	CL_p	Liver Concentration	CL_{bile}
	μg · min/ml	*ml/kg*	*ml/min/kg*	*ng/g liver*	*ml/min/kg*
SD rat	58.9 ± 9.1	76.3 ± 7.0	17.8 ± 2.5	1.41 ± 0.22	12.5 ± 1.0
EHBR	991 ± 32**	49.0 ± 0.8*	1.01 ± 0.03**	3.45 ± 0.19**	0.283 ± 0.010**

* $P < 0.05$, ** $P < 0.01$.

transporter-mediated drug-drug interactions. This kind of information may make it possible to predict the pharmacokinetics and subsequent pharmacological effects and side effects of drugs under certain conditions.

Next, to identify which transporters are involved in the biliary elimination of valsartan, we investigated the transcellular transport of valsartan in MDCKII cells coexpressing OATP1B1/MDR1, OATP1B1/MRP2, and OATP1B1/BCRP. As a result, the basal-to-apical transcellular transport of valsartan in OATP1B1/MRP2 double transfectant was the largest among three kinds of double transfected cells, whereas that in OATP1B1/MDR1 transfectant was slightly observed, and any significant transport could not be observed in OATP1B1/BCRP transfectant (Fig. 5). In parallel, we observed significant vectorial transport of estradiol-17β-glucuronide in OATP1B1/MDR1, OATP1B1/MRP2, and OATP1B1/BCRP double transfected cells at the same level as in a previous report (Matsushima et al., 2005). The ratio of the basal-to-apical transport to that in the opposite direction in OATP1B1/MRP2 cells was the highest among these double transfectants in the case of estradiol-17β-glucuronide and pravastatin (Matsushima et al., 2005), which were reported to be excreted mainly via MRP2, judged from the impairment of the biliary excretion in EHBR, an Mrp2-deficient rat (Yamazaki et al., 1997; Morikawa et al., 2000). These results suggest that valsartan is also mainly excreted by MRP2. We observed the saturation of transcellular transport in OATP1B1/MRP2 double transfectants with a K_m value of 27.5 μM (Fig. 6a; Table. 4). This K_m value is smaller than that of the efflux transport across the apical membrane (PS_{apical}) (99.0 μM) (Fig. 6b; Table. 4). From a kinetic viewpoint, if the intrinsic efflux clearance across the apical membrane, on which efflux transporters are over-expressed in MDCKII cells, is larger than that across the basal membrane, the transcellular clearance is almost equal to the uptake clearance. Therefore, the K_m value of transcellular transport represents that of OATP1B1-mediated uptake clearance. From our results, the K_m value of transcellular transport was greater than that of uptake by OATP1B1 in HEK293 cells. This discrepancy may be due to the fact that the host cells are different or the uptake process is not a rate-limiting step for the transcellular transport of valsartan. We also checked the ATP-dependent uptake of valsartan in MRP2-expressing membrane vesicles and found time-dependent saturable uptake (Fig. 7). The K_m value obtained from membrane vesicles is smaller than that of PS_{apical} in OATP1B1/MRP2 double transfectants. This is reasonable because we did not estimate the unbound intracellular concentration of valsartan in double transfectants, and the K_m value normalized by the unbound concentration should be lower than the current value.

In addition, we examined the biliary excretion of intravenously administered valsartan in SD rats and EHBRs, in which the MRP2 expression is hereditarily defective. The elimination of valsartan from blood was drastically delayed in EHBRs compared with SD rats, and the biliary excretion clearance in EHBRs was 44 times lower than that in SD rats (Fig. 8), indicating that MRP2 is responsible for the biliary excretion of valsartan, at least in rats. The contribution of transporters might show a species difference. However, taking the results of the transcellular transport in double transfected cells and the ATP-dependent uptake in MRP2-expressing membrane vesicles into consideration, it appears that MRP2 also plays an important role in the biliary excretion in humans.

Further investigations will be required to determine the contribution of efflux transporters to the overall biliary excretion in humans by quantitative comparison of the relative expression levels of each transporter in double transfectants and human liver samples. Information about the contribution of each transporter to hepatic drug transport will be provided by clinical studies investigating the effect of genetic polymorphisms in certain transporters on the pharmacokinetics of different drugs.

In conclusion, we have demonstrated that both OATP1B1 and OATP1B3 are responsible transporters for the hepatic uptake of valsartan, and the efflux clearance of valsartan is mainly via MRP2.

Acknowledgments. We are grateful to Masaru Hirano (The University of Tokyo, Tokyo, Japan) for helpful advice and to Satoshi Kitamura (The University of Tokyo, Tokyo, Japan) for supporting our experiments. We also express our great appreciation to Novartis Pharma AG (Basel, Switzerland) for providing us 3H-labeled and unlabeled valsartan and to Dr. Yuko Tsukamoto and Dr. Ryosei Kawai (Novartis Pharma K.K., Tokyo, Japan) for fruitful discussion.

References

Abe T, Unno M, Onogawa T, Tokui T, Kondo TN, Nakagomi R, Adachi H, Fujiwara K, Okabe M, Suzuki T, et al. (2001) LST-2, a human liver-specific organic anion transporter, determines methotrexate sensitivity in gastrointestinal cancers. *Gastroenterology* **120**:1689–1699.

Chandra P and Brouwer KL (2004) The complexities of hepatic drug transport: current knowledge and emerging concepts. *Pharm Res (NY)* **21**:719–735.

Colussi DM, Parisot C, Rossolino ML, Brunner LA, and Lefevre GY (1997) Protein binding in plasma of valsartan, a new angiotensin II receptor antagonist. *J Clin Pharmacol* **37**:214–221.

Evers R, Kool M, van Deemter L, Janssen H, Calafat J, Oomen LC, Paulusma CC, Oude Elferink RP, Baas F, Schinkel AH, et al. (1998) Drug export activity of the human canalicular multispecific organic anion transporter in polarized kidney MDCK cells expressing cMOAT (MRP2) cDNA. *J Clin Investig* **101**:1310–1319.

Flesch G, Muller P, and Lloyd P (1997) Absolute bioavailability and pharmacokinetics of valsartan, an angiotensin II receptor antagonist, in man. *Eur J Clin Pharmacol* **52**:115–120.

Hagenbuch B and Meier PJ (2004) Organic anion transporting polypeptides of the OATP/SLC21 family: phylogenetic classification as OATP/SLCO superfamily, new nomenclature and molecular/functional properties. *Pflueg Arch Eur J Physiol* **447**:653–665.

Hirano M, Maeda K, Shitara Y, and Sugiyama Y (2004) Contribution of OATP2 (OATP1B1) and OATP8 (OATP1B3) to the hepatic uptake of pitavastatin in humans. *J Pharmacol Exp Ther* **311**:139–146.

Hirano M, Maeda K, Shitara Y, and Sugiyama Y (2006) Drug-drug interaction between pitavastatin and various drugs via OATP1B1. *Drug Metab Dispos* **34**:1229–1236.

Hirouchi M, Suzuki H, Itoda M, Ozawa S, Sawada J, Ieiri I, Ohtsubo K, and Sugiyama Y (2004) Characterization of the cellular localization, expression level and function of SNP variants of MRP2/ABCC2. *Pharm Res (NY)* **21**:742–748.

Hsiang B, Zhu Y, Wang Z, Wu Y, Sasseville V, Yang WP, and Kirchgessner TG (1999) A novel human hepatic organic anion transporting polypeptide (OATP2). Identification of a liver-specific human organic anion transporting polypeptide and identification of rat and human hydroxymethylglutaryl-CoA reductase inhibitor transporters. *J Biol Chem* **274**:37161–37168.

Ishiguro N, Maeda K, Kishimoto W, Saito A, Harada A, Ebner T, Roth W, Igarashi T, and Sugiyama Y (2006) Predominant contribution of OATP1B3 to the hepatic uptake of telmisartan, an angiotensin II receptor antagonist, in humans. *Drug Metab Dispos* **34**: 1109–1115.

Kullak-Ublick GA, Ismair MG, Stieger B, Landmann L, Huber R, Pizzagalli F, Fattinger K, Meier PJ, and Hagenbuch B (2001) Organic anion-transporting polypeptide B (OATP-B) and its functional comparison with three other OATPs of human liver. *Gasteroenterology* **120**: 525–533.

Lowry OH, Rosebrough NJ, Farr AL, and Randall RJ (1951) Protein measurement with the Folin phenol reagent. *J Biol Chem* **193**:265–267

Matsushima S, Maeda K, Kondo C, Hirano M, Sasaki M, Suzuki H, and Sugiyama Y (2005) Identification of the hepatic efflux transporters of organic anions using double transfected MDCKII cells expressing human OATP1B1/MRP2, OATP1B1/MDR1 and OATP1B1/BCRP. *J Pharmacol Exp Ther* **314**:1059–1067.

Morikawa A, Goto Y, Suzuki H, Hirohashi T, and Sugiyama Y (2000) Biliary excretion of 17beta-estradiol 17beta-D-glucuronide is predominantly mediated by cMOAT/MRP2. *Pharm Res (NY)* **17**:546–552.

Nakai D, Nakagomi R, Furuta Y, Tokui T, Abe T, Ikeda T, and Nishimura K (2001) Human liver-specific organic anion transporter, LST-1, mediates uptake of pravastatin by human hepatocytes. *J Pharmacol Exp Ther* **297**:861–867.

Nishizato Y, Ieiri I, Suzuki H, Kimura M, Kawabata K, Hirota T, Takane H, Irie S, Kusuhara H, Urasaki Y, et al. (2003) Polymorphisms of OATP-C (SLC21A6) and OAT3 (SLC22A8) genes: consequences for pravastatin pharmacokinetics. *Clin Pharmacol Ther* **73**:554–565.

Shimizu M, Fuse K, Okudaira K, Nishigaki R, Maeda K, Kusuhara H, and Sugiyama Y (2005) Contribution of OATP (organic anion-transporting polypeptide) family transporters to the hepatic uptake of fexofenadine in humans. *Drug Metab Dispos* **33**:1477–1481.

Shitara Y, Itoh T, Sato H, Li AP, and Sugiyama Y (2003a) Inhibition of transporter-mediated hepatic uptake as a mechanism for drug-drug interaction between cerivastatin and cyclosporin A. *J Pharmacol Exp Ther* **304**:610–616.

Shitara Y, Li AP, Kato Y, Lu C, Ito K, Itoh T, and Sugiyama Y (2003b) Function of uptake transporters for taurocholate and estradiol 17beta-D-glucuronide in cryopreserved human hepatocytes. *Drug Metab Pharmacokinet* **18**:33–41.

Tamai I, Nezu J, Uchino H, Sai Y, Oku A, Shimane M, and Tsuji A (2000) Molecular identification and characterization of novel members of the human organic anion transporter (OATP) family. *Biochem Biophys Res Commun* **273**:251–260.

Vavricka SR, Van Montfoort J, Ha HR, Meier PJ, and Fattinger K (2002) Interactions of rifamycin SV and rifampicin with organic anion uptake systems of human liver. *Hepatology* **36**:164–172.

Waldmeier F, Flesch G, Muller P, Winkler T, Kriemler HP, Buhlmayer P, and De Gasparo M (1997) Pharmacokinetics, disposition and biotransformation of [14C]-radiolabelled valsartan in healthy male volunteers after a single oral dose. *Xenobiotica* **27**:59–71.

Yamaoka K, Tanigawara Y, Nakagawa T, and Uno T (1981) A pharmacokinetic analysis program (MULTI) for microcomputer. *J Pharmacobio-Dyn* **4**:879–885.

Yamazaki M, Akiyama S, Ni'inuma K, Nishigaki R, and Sugiyama Y (1997) Biliary excretion of pravastatin in rats: contribution of the excretion pathway mediated by canalicular multispecific organic anion transporter. *Drug Metab Dispos* **25**:1123–1129.

Address correspondence to: Dr. Yuichi Sugiyama, Department of Molecular Pharmacokinetics, Graduate School of Pharmaceutical Sciences, The University of Tokyo, 7-3-1 Hongo, Bunkyo-ku, Tokyo, 113-0033 Japan. E-mail: sugiyama@mol.f.u-tokyo.ac.jp

0026-895X/06/7003-887–896
MOLECULAR PHARMACOLOGY
U.S. Government work not protected by U.S. copyright
Mol Pharmacol 70:887–896, 2006

Vol. 70, No. 3
25494/3137121
Printed in U.S.A.

Regulation of the Expression of Human Organic Anion Transporter 3 by Hepatocyte Nuclear Factor 1α/β and DNA Methylation[S]

Ryota Kikuchi, Hiroyuki Kusuhara, Naka Hattori, Kunio Shiota, Insook Kim, Frank J. Gonzalez, and Yuichi Sugiyama

Department of Molecular Pharmacokinetics, Graduate School of Pharmaceutical Sciences (R.K., H.K., Y.S.), and Laboratory of Cellular Biochemistry, Department of Animal Resource Sciences/Veterinary Medical Sciences (N.H., K.S.), University of Tokyo, Tokyo, Japan; and Laboratory of Metabolism, National Cancer Institute, National Institutes of Health, Bethesda, Maryland (I.K., F.J.G.)

Received April 8, 2006; accepted June 20, 2006

ABSTRACT

Human organic anion transporter 3 (hOAT3/SLC22A8) is predominantly expressed in the proximal tubules of the kidney and plays a major role in the urinary excretion of a variety of organic anions. The promoter region of hOAT3 was characterized to elucidate the mechanism underlying the tissue-specific expression of hOAT3. The minimal promoter of hOAT3 was identified to be located approximately 300 base pairs upstream of the transcriptional start site, where there are canonical TATA and hepatocyte nuclear factor (HNF1) binding motifs, which are conserved in the rodent Oat3 genes. Transactivation assays revealed that HNF1α and HNF1β markedly increased hOAT3 promoter activity, where the transactivation potency of HNF1β was lower than that of HNF1α. Mutations in the HNF1 binding motif prevented the transactivation. Electrophoretic mobility shift assays demonstrated binding of the HNF1α/HNF1α homodimer or HNF1α/HNF1β heterodimer to the hOAT3 promoter. It was also demonstrated that the promoter activity of hOAT3 is repressed by DNA methylation. Moreover, the expression of hOAT3 was activated de novo by forced expression of HNF1α alone or both HNF1α and HNF1β together with the concomitant DNA demethylation in human embryonic kidney 293 cells that lack expression of endogenous HNF1α and HNF1β, whereas forced expression of HNF1β alone could not activate the expression of hOAT3. This suggests a synergistic action of the HNF1α/HNF1α homodimer or HNF1α/HNF1β heterodimer and DNA demethylation for the constitutive expression of hOAT3. These results indicate that the tissue-specific expression of hOAT3 might be regulated by the concerted effect of genetic (HNF1α and HNF1β) and epigenetic (DNA methylation) factors.

Tubular secretion plays a significant role in the urinary excretion of many compounds together with filtration in the glomeruli. Cumulative evidence suggests that organic anion transporter 1 (OAT1/SLC22A6) and organic anion transporter 3 (OAT3/SLC22A8) are predominantly involved in the tubular secretion of anionic drugs and drug metabolites as well as endobiotics at the basolateral membrane of the kidney proximal tubules (Van Aubel et al., 2000; Hasegawa et al., 2002, 2003; Robertson and Rankin, 2005; Sekine et al., 2006). Generation of Oat1 and Oat3 null mice confirmed an essential role for these transporters in the renal transport (Sweet et al., 2002; Eraly et al., 2006). In contrast to the functional characterization of these transporters, the regulatory mechanism of the basal expression of OAT1 and OAT3 remains to be elucidated.

In the present study, we focused on hepatocyte nuclear factor 1 (HNF1), consisting of two isoforms, HNF1α and HNF1β, as a key regulator of OAT3 expression. HNF1 is a homeodomain-containing factor that is expressed in the epithelia of a variety of organs, including liver, kidney, intestine, stomach, and pancreas (Blumenfeld et al., 1991; Mendel and Crabtree, 1991; Tronche and Yaniv, 1992). In the kidney, expression of HNF1α is confined to the proximal tubules,

This work was supported by a Health and Labor Sciences research grant from the Ministry of Health, Labor and Welfare for the Research on Advanced Medical Technology.

Article, publication date, and citation information can be found at http://molpharm.aspetjournals.org.

doi:10.1124/mol.106.025494.

[S] The online version of this article (available at http://molpharm.aspetjournals.org) contains supplemental material.

ABBREVIATIONS: OAT, organic anion transporter; HNF1, hepatocyte nuclear factor 1; h, human; PCR, polymerase chain reaction; m, mouse; EMSA, electrophoretic mobility shift assay; HEK, human embryonic kidney; DTT, dithiothreitol; 5azadC, 5-aza-2′-deoxycytidine; wt, wild-type HNF1 sequence; per, perfect consensus sequence; mut, mutated consensus sequence; RT, reverse transcription; GAPDH, glyceraldehyde-3-phosphate dehydrogenase; TBS-T, Tris-buffered saline/0.05% Tween 20; nt, nucleotide(s).

whereas that of HNF1β is observed along the tubular epithelial cells throughout the entire nephron (Lazzaro et al., 1992; Pontoglio et al., 1996). HNF1 is functionally composed of three domains: an N-terminal dimerization domain, a homeobox-like DNA-binding domain, and a C-terminal transactivation domain. Both the dimerization domain and the DNA-binding domain of HNF1α and HNF1β show high homologies, enabling them to form heterodimers as well as homodimers and to recognize the same DNA sequences (Mendel et al., 1991). In contrast, their transactivation domains are more divergent, and HNF1α is a more potent transactivator than HNF1β (Rey-Campos et al., 1991).

HNF1α is involved in the regulation of a number of hepatic genes, including albumin, α1-antitrypsin, and α- and β-fibrinogen (Mendel and Crabtree, 1991; Tronche and Yaniv, 1992), and also some of the transporters expressed predominantly in liver (Jung et al., 2001; Shih et al., 2001). The importance of HNF1α in kidney proximal tubules has become apparent after studies using two lines of HNF1α-null mice as well as conventional in vitro studies (Pontoglio et al., 1996; Lee et al., 1998). One line of HNF1α-null mice suffers from renal Fanconi syndrome, a defect in renal proximal tubule reabsorption, leading to glucosuria, aminoaciduria, phosphaturia, and polyuria. Indeed, HNF1α plays an essential role in the expression of sodium glucose cotransporter 2 and sodium/phosphate cotransporter 1, which are involved in the reabsorption of filtered glucose and phosphate from the urine, respectively (Pontoglio et al., 2000; Cheret et al., 2002).

In contrast to HNF1α, the role of HNF1β in adult animals remains unclear, because the homologous inactivation of the HNF1β gene results in embryonic lethality at embryonic day 7.5 as a result of a defect in visceral endoderm differentiation (Barbacci et al., 1999; Coffinier et al., 1999). However, more recently, HNF1β was shown to be essential for the formation of a functional bile duct system and several hepatic metabolic functions, by means of the conditional gene-targeting technique (Coffinier et al., 2002). HNF1β is also involved in the regulation of kidney-specific Ksp-cadherin promoter (Bai et al., 2002), and kidney-specific inactivation of HNF1β leads to a renal polycystic phenotype (Gresh et al., 2004).

Because multiple CpG dinucleotides, primary targets of DNA methylation in the vertebrate genome, are located in the putative promoter region of hOAT3 (Fig. 1), we also focused on the role of DNA methylation in regulation of hOAT3 expression. DNA methylation is one of the mechanisms underlying the epigenetic control of gene expression (Bird, 2002). Methylation of the CpG dinucleotides in the promoter region can evoke the condensed structure of chromatin in the neighboring region through the recruitment of chromatin remodeling factors, such as methyl CpG binding proteins and histone deacetylases, which prevents transactivation by most of the transcription factors. Therefore, there is an inverse correlation between gene expression and DNA methylation in the promoter region. During the last decade, the role of DNA methylation in mammalian embryogenesis, differentiation, and progression of cancer has been highlighted. More recently, DNA methylation has been recognized to regulate the tissue-specific expression of many genes (Shiota, 2004). Whether these epigenetic mechanisms are involved in the regulation of transporter genes has remained largely unknown.

In the present study, we report the isolation of the hOAT3 promoter and demonstrate the involvement of HNF1α and HNF1β in basal transcriptional activity. In addition, these studies revealed that DNA methylation is involved in the gene suppression of hOAT3, and transcriptional activation of hOAT3 by HNF1α and HNF1β requires concomitant DNA demethylation of the promoter.

Materials and Methods

Materials. All reagents were purchased from Wako Pure Chemicals (Osaka, Japan) unless stated otherwise.

Isolation of the 5′-Flanking Region of the hOAT3 and mOat3 Gene. The transcriptional start site of the hOAT3 gene was identified using the public database Database of Transcriptional Start Sites (http://dbtss.hgc.jp/), with the ref sequence identification for hOAT3 (GenBank accession number NM_004254). DNA fragments of varying length from the 5′-flanking region of the hOAT3 gene were generated by polymerase chain reaction (PCR) using human genomic DNA as a template and the following primer sets:

Fig. 1. Multiple alignment of the putative proximal promoter of human, mouse, and rat OAT3. Nucleotide sequences of the 5′-flanking region of human (top), mouse (middle), and rat (bottom) OAT3 genes were aligned using Genetyx-Mac version 10 (Genetyx, Tokyo, Japan), so that the maximal homology of sequences among species could be obtained. Nucleotide numberings are relative to the transcriptional start sites (nt +1, arrow). Homologous sequences among species are boxed. Representative consensus binding motifs for putative regulatory elements are shaded with the respective transcription factors given above the sequence, and CpG dinucleotides in each sequence are reverse-colored.

forward, −1471, −644, or −308, and reverse +6 (Table 1). The primers were designed according to the sequence of the 5′-flanking region of the hOAT3 gene, and the number indicates the position of the primers relative to the transcriptional start site. The forward primers contained an artificial KpnI site and the reverse primers contained an artificial HindIII site. The resulting PCR products (−1471/+6, −644/+6, and −308/+6) were digested with KpnI and HindIII after subcloning into pGEM-T Easy vector (Promega, Madison, WI) and ligated into pGL3-Basic vector (Promega) predigested with KpnI and HindIII, yielding the following promoter constructs: −1471/+6-Luc, −644/+6-Luc, and −308/+6-Luc. The −35/+6-Luc construct was generated by in vitro annealing of the sense (−35/+6) and antisense (+6/−35) oligonucleotides (Table 1) followed by ligation into the pGL3-Basic vector that had been predigested with KpnI and HindIII. The mOat3 promoter fragment was PCR-amplified from mouse genomic DNA using the following primers: forward (−156) and reverse (+6) (Table 1). The amplified product was ligated into the pGL3-Basic vector as in the case of hOAT3, yielding the mOat3-Luc promoter construct. The sequence identity of all the constructs with the respective genomic sequences was verified by DNA sequencing. Plasmid DNA was prepared using the GenElute Plasmid Midiprep kit (Sigma-Aldrich, St. Louis, MO).

Plasmid Constructions. To generate HNF1α and HNF1β expression vectors, the coding regions of human HNF1α and HNF1β were amplified by PCR using primers containing HindIII and EcoRI restriction sites and inserted into the same sites of pcDNA3.1(+) vector (Invitrogen, Carlsbad, CA). The sequences of primers used for the amplification of HNF1α and HNF1β are listed in Table 1. The entire sequences were verified by DNA sequencing.

Site-Directed Mutagenesis. The mutated promoter fragment (−308/+6-HNF1mut) having a 4-base pair disrupted HNF1 motif was generated using the QuikChange XL site-directed mutagenesis kit (Stratagene, La Jolla, CA) using internal mutated oligonucleotides (Table 1). The introduction of the mutations was verified by DNA sequencing.

In Vitro Methylation of Plasmid DNA. Reporter constructs of the hOAT3 promoter were methylated in vitro with 3 U of SssI methylase (New England Biolabs, Beverly, MA) for each microgram of DNA in the presence of 160 μM *S*-adenosylmethionine at 37°C for 3 h. Completion of the methylation was confirmed by resistance to HpaII digestion (data not shown).

Cell Culture and Transfections. HepG2 and Caco-2 cell lines were maintained in a culture medium consisting of Dulbecco's modified Eagle's medium with 4500 mg/l glucose (Invitrogen) supplemented with 10% fetal bovine serum (Sigma-Aldrich), nonessential amino acids, 100 U/ml penicillin, and 100 μg/ml streptomycin (Invitrogen). The HEK293 cell line was maintained in a culture medium consisting of Dulbecco's modified Eagle's medium with 1000 mg/l glucose supplemented with 10% fetal bovine serum, 100 U/ml penicillin, and 100 μg/ml streptomycin. Cells were seeded in 24-well culture plates (0.5×10^5 cells/well) 1 day before transfection. HepG2 and Caco-2 cells were transfected with 0.5 μg of the corresponding promoter construct and 0.05 μg of the internal standard pRL-SV40 vector (Promega) to normalize the transfection efficiency using Lipofectamine 2000 (Invitrogen) according to the manufacturer's instructions. HEK293 cells were transfected with 0.5 μg of the corresponding promoter and 0.05 μg of pRL-SV40 using FuGENE 6 (Roche Diagnostics, Indianapolis, IN). For cotransfection assays with HEK293 cells, 0 to 0.5 μg of HNF1α and HNF1β expression vectors or empty pcDNA3.1(+) vector was added to the transfection reaction. Then, 48 h after transfection, cells were lysed with passive lysis buffer, and the luciferase activities were assayed using the dual-luciferase reporter system (Promega) and quantified in a Lumat LB 9507 luminometer (Berthold, Bad Wildbad, Germany). The promoter activity was measured as the relative light units of firefly luciferase per unit of *Renilla reniformis* luciferase.

TABLE 1

Oligonucleotides used for the production of promoter fragments, plasmid construction, mobility shift assays, site-directed mutagenesis, RT-PCR, and quantitative PCR

Regarding the oligonucleotides used for the mobility shift assays and site-directed mutagenesis, the HNF1 recognition motif in the hOAT3 promoter region is underlined. Bold type indicates the difference in the sequence of the per and mut compared with wt sequence found in the hOAT3 promoter.

Oligonucleotide	Orientation	Sequence (5′ to 3′)
Primers and oligonucleotides used for cloning of 5′-flanking regions		
hOAT3		
−1471	Forward	CGGGGTACCGGAACAGAGAGGTAAAGGC
−644	Forward	CGGGGTACCGAGAGAAGCCTGTCCATTG
−308	Forward	CGGGGTACCGATTCCTTCCCAGAATCTCC
+6	Reverse	CCCAAGCTTCAAGCTGTGTTTGTGCCTCC
−35/+6	Sense	CCCTTATATAAGCCCCCCTGGGGGAGGCACAAACACAGCTTGA
+6/−35	Antisense	AGCTTCAAGCTGTGTTTGTGCCTCCCCCAGGGGGGCTTATATAAGGGGTAC
mOat3		
−156	Forward	CGGGGTACCATCAACAGCCTTGGCTGAGG
+6	Reverse	CCCAAGCTTCAAGCTGTTTGTGTCTCC
Primers used for cloning of HNF1α and HNF1β		
HNF1α	Forward	AAGCTTGCCATGGTTTCTAAACTGAGCC
	Reverse	GAATTCTGGTTACTGGGAGGAAGAGGCC
HNF1β	Forward	AAGCTTGAAAATGGTGTCCAAGCTCACG
	Reverse	GAATTCGGCATCACCAGGCTTGTAGAGG
Oligonucleotides used for construction of EMSA probe and competitor or site-directed mutagenesis		
wt	Sense	CGCAAAAGAAAGTCAAACATTAGCCCGGGAAACAGC
per	Sense	CGCAAAAGAAAGTTAATCATTAACCCGGGAAACAGC
mut	Sense	CGCAAAAGAAAGTCACACATCGCCCCGGGAAACAGC
Primers used for RT-PCR or quantitative PCR		
hOAT3	Forward	GGCAGGTATACTGATTGGAG
	Reverse	TCCACCAGGATGATAGGAAG
HNF1α	Forward	TGGGTCCTACGTTCACCAAC
	Reverse	TCTGCACAGGTGGCATGAGC
HNF1β	Forward	TGCACAAAGCCTCAACACCT
	Reverse	GTTGGTGAGTGTACTGATGC
GAPDH	Forward	AATGACCCCTTCATTGAC
	Reverse	TCCACGACGTACTCAGCGC

Preparation of Nuclear Extracts. Nuclear extracts were prepared from 1.0×10^7 of HepG2, Caco-2, and HEK293 cells. Cell centrifugation and the subsequent steps to recover the nuclear proteins were all performed at 4°C. Cells were scraped off the plates, suspended in 0.5 ml of phosphate-buffered saline, and centrifuged at 1500*g* for 5 min. The cellular pellet was resuspended in 150 μl of buffer A (10 mM HEPES, pH 7.9, 10 mM KCl, 0.2 mM EDTA, 0.4% Nonidet P-40, 1 mM DTT, 0.5 mM phenylmethylsulfonyl fluoride, and 1% protease inhibitor cocktail; Sigma-Aldrich). After a 10-min incubation on ice, cells were centrifuged at 4°C and 3000 rpm for 5 min. The pellet was resuspended in 150 μl of buffer A and centrifuged at 4°C and 3000 rpm for 5 min, and this process was repeated twice. The supernatant was removed, and the nuclear pellet was resuspended in 200 μl of buffer B (20 mM HEPES, pH 7.9, 400 mM NaCl, 2 mM EDTA, 1 mM DTT, 0.5 mM phenylmethylsulfonyl fluoride, and 1% protease inhibitor cocktail) and incubated on ice for 30 min. The tube was centrifuged at 4°C and 10,000 rpm for 20 min, and the supernatant was recovered as the nuclear extract. Protein concentrations were measured by the method of Lowry et al. (1951).

Electrophoretic Mobility Shift Assay. The double-stranded oligonucleotide probes were obtained by hybridizing single-stranded complementary oligonucleotides with sense sequences as shown in Table 1. Digoxigenin-11-ddUTP was incorporated into each 3′ end using a Dig Gel Shift kit, 2nd Generation (Roche Diagnostics). Sequence wt corresponds to the wild-type HNF1 sequence found in the hOAT3 promoter, and per corresponds to the perfect consensus sequence for HNF1, whereas mut denotes the wild-type sequence mutated within the HNF1 recognition motif. For EMSA, 5 μg of nuclear extracts from HepG2, Caco-2, and HEK293 cells was incubated at room temperature for 15 min with 30 fmol of digoxigenin-labeled probe, 2 μg of poly(dI-dC), and 0.1 μg of poly-L-lysine in 20 μl of 20 mM HEPES, pH 7.6, 1 mM EDTA, 10 mM $(NH_4)_2SO_4$, 1 mM DTT, 2% (w/v) Tween 20, and 30 mM KCl. For competition assays, a 25-fold excess of unlabeled dimerized oligonucleotides was added. For supershift experiments, 1 μg of antibody against HNF1α or HNF1β (Santa Cruz Biotechnology, Inc., Santa Cruz, CA) was added to the reaction mixture. Reactions were analyzed by electrophoresis through Novex 6% DNA retardation gels (Invitrogen). After electrotransfer to a positively charged nylon membrane (Roche Diagnostics), bands were detected nonisotopically with a Dig Gel Shift kit, 2nd Generation, according to the manufacturer's instructions.

5-Aza-2′-deoxycytidine Treatment and Analysis of hOAT3 Expression by Reverse Transcription-PCR. Before the treatment with 5-aza-2′-deoxycytidine (5azadC) (DNA methylation inhibitor; Sigma-Aldrich), HepG2, Caco-2, and HEK293 cells were precultured for 24 h and then cultured for 72 h in medium containing 0, 1, 10, or 100 μM 5azadC. To examine the synergetic effect of the expression of HNF1α or HNF1β and DNA demethylation, HEK293 cells were plated in 24-well plates (0.5×10^5 cells/well) 1 day before transient transfection of 0 to 0.5 μg of HNF1α expression vector, HNF1β expression vector, or empty pcDNA3.1(+) vector. The transfection was performed using FuGENE 6 according to the manufacturer's instructions. After 12 h, the cells were treated with 0 or 100 μM 5azadC, cultured for 48 h, and then subjected to RNA isolation. Total RNA was prepared from cells by a single-step guanidium thiocyanate procedure using ISOGEN (Nippon Gene, Toyama, Japan). The RNA was then reverse-transcribed using a random-nonamer primer (Takara, Shiga, Japan). PCR was performed with the forward and reverse primers listed in Table 1 to detect the partial fragments of hOAT3, HNF1α, HNF1β, and GAPDH cDNA. PCR was performed under the following conditions: 94°C for 2 min; 40 cycles for hOAT3, 30 cycles for HNF1α and HNF1β, and 25 cycles for GAPDH of 94°C for 30 s, 55°C for 30 s, and 72°C for 1 min; final extension 72°C for 5 min.

Quantitative PCR. To quantify the mRNA expression of HNF1α and HNF1β in HepG2, Caco-2, and HEK293 cells, real-time quantitative PCR was performed using a LightCycler and the appropriate software (version 3.53; Roche Diagnostics) according to the manufacturer's instructions. cDNA used for the quantification was prepared as described above. Primers for HNF1α and HNF1β used in this study are shown in Table 1.

PCR was performed using a SYBR Premix Ex *Taq* (perfect real time) (Takara). The protocol for PCR was as follows: 95°C for 30 s, 40 cycles of 95°C for 5 s, 55°C for 10 s, and 72°C for 15 s. A standard curve was generated by dilutions of the target PCR product, which had been purified and had its concentration measured. To confirm the amplification specificity, the PCR products were subjected to a melting curve analysis. The mRNA expression of HNF1α and HNF1β in each cell line was normalized by the mRNA expression of GAPDH.

Western Blotting. Nuclear extracts prepared from HepG2 or Caco-2 cells were subjected to Western blot analysis to confirm the expression of HNF1α and HNF1β at protein levels. In this, 30 μg of nuclear proteins was electrophoresed on 10% SDS-polyacrylamide gel with a 4.4% stacking gel. Separated proteins were transferred to a polyvinylidene difluoride membrane using a blotter at 15 V for 1 h. The membrane was blocked with Tris-buffered saline/0.05% Tween 20 (TBS-T) and 5% skimmed milk for 1 h at room temperature and subsequently incubated with an antibody against HNF1α or HNF1β (1:2000) at 4°C overnight. After washing three times with TBS-T for 5 min, the membrane was allowed to bind a horseradish peroxidase-labeled donkey anti-goat IgG (Chemicon International, Temecula, CA) diluted 1:5000 in TBS-T for 1 h at room temperature and detected using ECL Plus (GE Healthcare, Little Chalfont, Buckinghamshire, UK).

Results

Computational Analysis of the Potential Transcription Factor Binding Sites in hOAT3, mOat3, and rOat3 Minimal Promoters. Sequence homologies to known gene regulatory elements in the hOAT3 5′-flanking region up to approximately nt −300 relative to the transcription start site were identified by a computer-based approach using Mat Inspector (http://www.genomatix.de/) (Fig. 1). Several potential transcription factor recognition sites were found in this region, including a TATA motif at nt −32 to −27, an HNF1 binding motif at nt −65 to −53, a cAMP response element-binding protein binding motif at nt −87 to −80, and a signal transducer and activator of transcription 5 binding motif at nt −302 to −294. In addition, there are 13 CpG dinucleotides in this region, which may be potential DNA methylation sites (Fig. 1). A homologous sequence to the hOAT3 5′-flanking region in the mouse and rat Oat3 genomic locus was obtained from the National Center for Biotechnology Information genome database. The transcriptional start site of mOat3 and rOat3 gene was suggested based on the high homology (approximately 70%) to the hOAT3 5′-flanking region (Fig. 1). The TATA motif and HNF1 motif were also found in the mOat3 and rOat3 putative promoters.

Analysis of Basal hOAT3 Gene Promoter Activity. To determine the minimal region of the hOAT3 proximal promoter required for its promoter activity, a series of deleted promoter constructs (−1471/+6-Luc, −644/+6-Luc, −308/+6-Luc, and −35/+6-Luc) were transfected into three kinds of human-derived cell lines (HepG2, Caco-2, and HEK293), and the luciferase activity in each cell line was measured (Fig. 2). The transfection of −1471/+6, −644/+6, and −308/+6 constructs resulted in increased luciferase activity compared with the promoterless pGL3-Basic plasmid in all cell lines, whereas no significant luciferase activity was observed after transfection of the −35/+6 construct. These

results suggest that −308 to +6 of the hOAT3 5′-flanking region can act as a minimal promoter. The luciferase activity of the −644/+6 construct was much lower than that of the −308/+6 construct only in HepG2 cells, suggesting the existence of some negative regulatory elements between −644 and −308 in this liver-derived tumor cell line.

Expression Level of HNF1α and HNF1β in HepG2, Caco-2, and HEK293 Cells. Real-time quantitative PCR revealed that the expression level of HNF1β in HepG2 cells was 27% that of HNF1α (Fig. 3A). The levels of HNF1α and HNF1β mRNA in Caco-2 cells were 73 and 55% that of HNF1α in HepG2 cells, respectively. In contrast, neither HNF1α nor HNF1β was detected in HEK293 cells. Western blot analysis with nuclear extracts from HepG2 or Caco-2 cells demonstrated that in HepG2 cells, HNF1α is predominantly expressed at the protein level, whereas in Caco-2 cells, both HNF1α and HNF1β are expressed (Fig. 3B).

Mutagenesis of the HNF1 Binding Motif. To investigate the functional importance of the HNF1 binding motif in the hOAT3 promoter region for the basal promoter activity, mutations in this motif were introduced into the −308/+6-Luc construct, and the reporter activity was measured after transfection into HepG2, Caco-2, and HEK293 cells (Fig. 4). Mutations in the HNF1 binding motif attenuated the luciferase activity by approximately 50% compared with the wild-type construct in HepG2 and Caco-2 cells where endogenous HNF1α and HNF1β were detected by real-time quantitative PCR. In contrast, HNF1 motif disruption by site-directed mutagenesis had no effect on the transcriptional activity in HNF1α- and HNF1β-deficient HEK293 cells. These results confirm that the HNF1 binding motif in the hOAT3 promoter is functional.

Transactivation of the Promoter Activity by Exogenous Expression of HNF1α and/or HNF1β. The effect of exogenously expressed HNF1α and HNF1β on the hOAT3 promoter activity was investigated by cotransfection assays in HEK293 cells. As shown in Fig. 5, independent or simultaneous transfection of HNF1α and HNF1β enhanced the luciferase activity of the hOAT3 −308/+6 wild-type reporter construct (−308/+6-HNF1wt) compared with the pcDNA3.1(+)-transfected control. The luciferase activities of the promoterless pGL3-Basic or hOAT3 −308/+6 HNF1-mutated reporter construct (−308/+6-HNF1mut) were not stimulated by transfection of the HNF1α and/or HNF1β expression vectors. These results provide clear evidence that both HNF1α and HNF1β can transactivate the basal promoter activity of hOAT3 and that the effect is mediated by the intact HNF1 binding motif in the hOAT3 promoter. The luciferase activity of the wild-type reporter construct with the independent transfection of HNF1α is higher than that

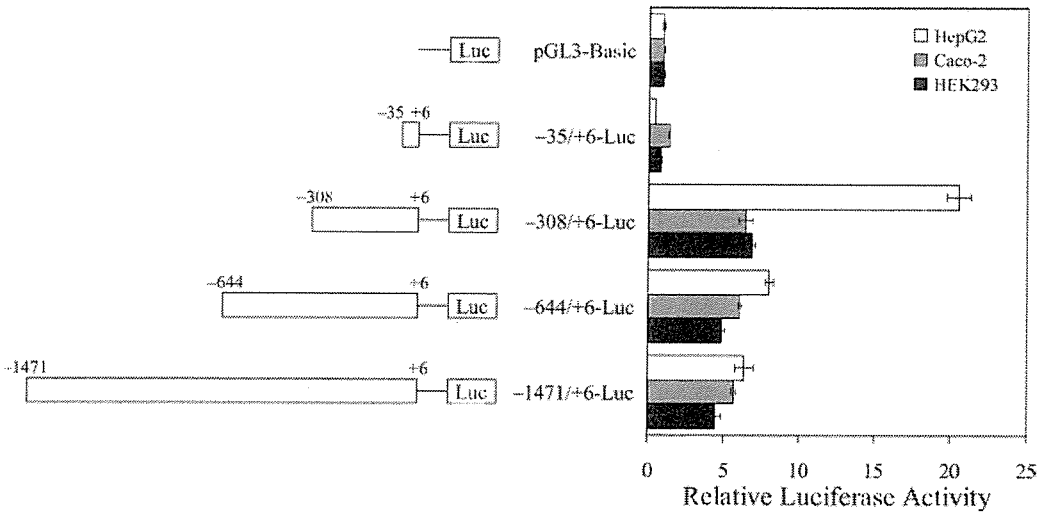

Fig. 2. Analysis of hOAT3 promoter function. HepG2 (white bars), Caco-2 (gray bars), and HEK293 cells (black bars) were transiently transfected with a series of deleted promoter constructs −35/+6-Luc, −308/+6-Luc, −644/+6-Luc, and −1471/+6-Luc, or a promoterless pGL3-Basic plasmid as described under *Materials and Methods*. Transfection efficiency was normalized by cotransfection of internal standard pRL-SV40. The promoter activity was measured as described under *Materials and Methods* and was shown as the factor of induction of luciferase over background activity measured in cells transfected with pGL3-Basic in each cell line. Results are presented as the mean ± S.E. of triplicate samples.

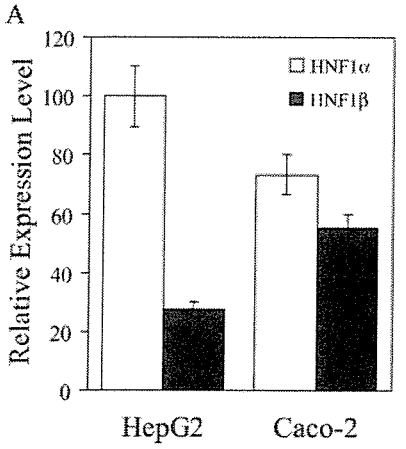

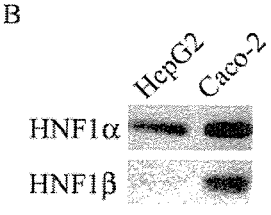

Fig. 3. Expression of HNF1α and HNF1β in HepG2, Caco-2, and HEK293 cells. A, mRNA expression of HNF1α and HNF1β was measured by real-time quantitative PCR using specific primers (Table 1), and the data were normalized by the mRNA expression of GAPDH. The relative expression level of HNF1α (white columns) and HNF1β (black columns) in each cell line was given as a ratio with respect to the mRNA expression of HNF1α in HepG2 cells which was taken as 100%. Results are presented as the mean ± S.E. of three samples. B, Western blotting was performed to investigate the protein expression of HNF1α and HNF1β. Nuclear extracts from HepG2 or Caco-2 cells were separated by SDS-polyacrylamide gel electrophoresis (10% separating gel), and HNF1α and HNF1β were detected as described under *Materials and Methods*.

with the independent transfection of HNF1β, indicating that the transactivation potency of HNF1β is lower than that of HNF1α. Simultaneous transfection of HNF1α and HNF1β yielded intermediate luciferase activity, which may be explained by the formation of a HNF1α/HNF1β heterodimer that enhances the promoter activity to the lesser degree than the HNF1α/HNF1α homodimer.

HNF1 Binds to the hOAT3 Promoter. EMSA was performed using the oligonucleotide probe corresponding to the −76/−41 region of the hOAT3 promoter, which includes the HNF1 binding motif and the nuclear extracts from HepG2, Caco-2, and HEK293 cells to show direct binding of HNF1α or HNF1β to the promoter (Fig. 6A). Incubation of the −76/−41 oligonucleotide probe with nuclear extracts from three cell lines resulted in three shifted bands (*a*, *b*, and *c*). The band *a* was observed when the probe was incubated with the nuclear extract from HepG2 cells (lane 2), and an additional band (band *b*) showing faster mobility was detected when the probe was incubated with the nuclear extracts from Caco-2 cells (lane 5). Band *c* was produced by incubation with the nuclear extract from each cell line (lanes 2, 5, and 8). The formation of bands *a* and *b* was abolished by an excess of unlabeled HNF1 consensus oligonucleotide (per) (lanes 3 and 6), but it was unaffected by the mutated oligonucleotide (mut) (lanes 4 and 7). These results suggest that the bands *a* and *b* can be ascribed to the binding of HNF1α or HNF1β to the −76/−41 oligonucleotide probe.

To confirm the specificity of HNF1 binding, supershift analysis was performed with HepG2 and Caco-2 nuclear extracts using a specific antibody to HNF1α or HNF1β (Fig. 6B). Band *a* was supershifted by the addition of an antibody to HNF1α but not by an antibody to HNF1β (lanes 3, 4, 6, and 7), whereas band *b* observed only in Caco-2 cells was supershifted by the addition of either of the antibodies (lanes 6 and 7). Thus, band *a* corresponds to HNF1α/HNF1α homodimer, and band *b* corresponds to HNF1α/HNF1β heterodimer. A previous report has shown that HNF1β/HNF1β homodimer migrating faster than HNF1α/HNF1β heterodimer may exist when both isoforms are present (Rey-Campos et al., 1991). However, in the present study, the formation of HNF1β/HNF1β homodimer was not clearly observed in Caco-2 cells where both isoforms were detected. The band *c* is ascribed to some nonspecific binding to the labeled probe, because this band was not abolished by the addition of unlabeled oligonucleotides. Taken together, these data suggest that the protein complex binding to the hOAT3 HNF1 motif in HepG2 cells is HNF1α/HNF1α homodimer and those in Caco-2 cells include HNF1α/HNF1β heterodimer as well as HNF1α/HNF1α homodimer. The difference in the band pattern is probably due to the different protein expression pattern of HNF1α and HNF1β in the two cell lines (Fig. 3B).

Transcriptional Activation of mOat3 Promoter by HNF1α and HNF1β. To investigate whether HNF1α or HNF1β is also involved in the promoter activity of mOat3, the proximal putative promoter of mOat3 was cloned into pGL3-Basic vector using the PCR-based approach, and the promoter activity of this reporter construct was measured in HepG2, Caco-2, and HEK293 cells. The luciferase activity of the mOat3 −156/+6 promoter construct (mOat3-Luc) was 6.5- and 3.6-fold higher than the promoterless pGL3-Basic plasmid in HepG2 and Caco-2 cells, respectively, whereas the activity in HEK293 cells was not significant (Supplemental Data A). Exogenous expression of HNF1α or HNF1β in HEK293 cells enhanced the promoter activity of mOat3 (Supplemental Data B). These observations suggest that the functional importance of HNF1α and HNF1β for the basal transcription of OAT3 genes is conserved among species.

Repression of hOAT3 Promoter Activity by DNA Methylation. To investigate the possible role of DNA methylation on the transcriptional repression of hOAT3, hOAT3 −308/+6 promoter construct was methylated in vitro; transfected into HepG2, Caco-2, and HEK293 cells; and the luciferase activity was measured. The transcriptional activity of hOAT3 was dramatically reduced by in vitro methylation of the promoter construct (Fig. 7). These data indicate that the

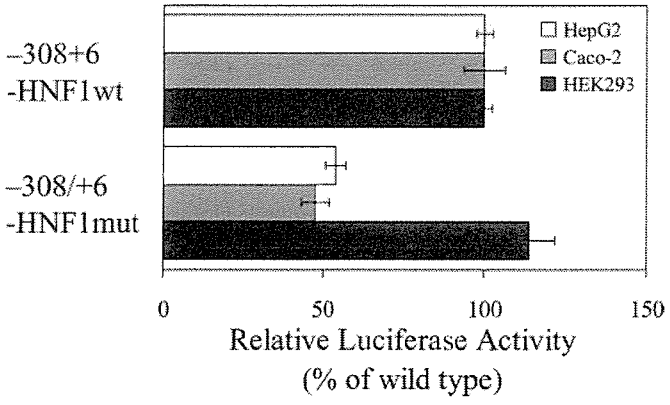

Fig. 4. Effect of mutations in the HNF1 binding motif on the hOAT3 promoter activity. HepG2 (white bars), Caco-2 (gray bars), and HEK293 cells (black bars) were transfected with wild-type (−308/+6-HNF1wt) or mutated (−308/+6-HNF1mut) promoter construct, and the luciferase activity was measured as described under *Materials and Methods*. The relative luciferase activity of the mutated construct is shown as a percentage of the wild-type construct in each cell line. Results are presented as the mean ± S.E. of triplicate samples.

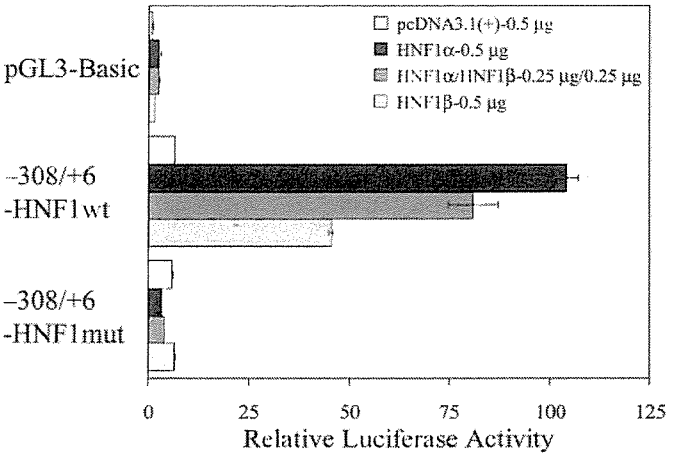

Fig. 5. Effect of exogenously expressed HNF1α and HNF1β on hOAT3 promoter function in HEK293 cells. HEK293 cells were transfected with wild type (−308/+6-HNF1wt) or mutated (−308/+6-HNF1mut) promoter construct, or a promoterless pGL3-Basic plasmid, together with 0.5 μg/well empty pcDNA3.1(+) vector (white bars), 0.5 μg/well HNF1α expression vector (black bars), 0.25 μg/well HNF1α and HNF1β expression vectors (gray bars), or 0.5 μg/well HNF1β expression vector (light gray bars). The luciferase activity was measured as described under *Materials and Methods* and was shown as the factor of induction over background activity measured in cells transfected with pGL3-Basic together with pcDNA3.1(+). Results are presented as the mean ± S.E. of triplicate samples.

expression of hOAT3 can be suppressed at a transcriptional level by DNA methylation.

Activation of hOAT3 Transcription by 5azadC Treatment in Nonexpressing Cell Lines. Expression of the endogenous hOAT3 gene in HepG2, Caco-2, and HEK293 cells is below the detection limit. To investigate whether the hOAT3 gene could be activated by DNA demethylation in these nonexpressing cell lines, the total RNA from each cell line treated with 5azadC, an inhibitor for DNA methyltransferases, was subjected to RT-PCR analysis. hOAT3 mRNA became detectable in Caco-2 cells after treatment with 5azadC in a concentration-dependent manner (Fig. 8A), whereas no induction of hOAT3 mRNA was observed in HepG2 or HEK293 cells (data not shown). In HEK293 cells, however, transient transfection of HNF1α alone or cotransfection of HNF1α and HNF1β followed by treatment with 100 μM 5azadC elicited de novo expression of hOAT3 mRNA, whereas transfection of HNF1β alone was not sufficient to induce hOAT3 expression (Fig. 8B). These data suggest that the repression mechanism of the hOAT3 gene in hOAT3-nonexpressing cells involves DNA methylation and that synergism between HNF1α or HNF1β expression and DNA demethylation may be required for the transcription of this gene.

Discussion

In the present study, the transcriptional regulation of the hOAT3 gene was characterized for the first time. The promoter region required for basal promoter activity was deter-

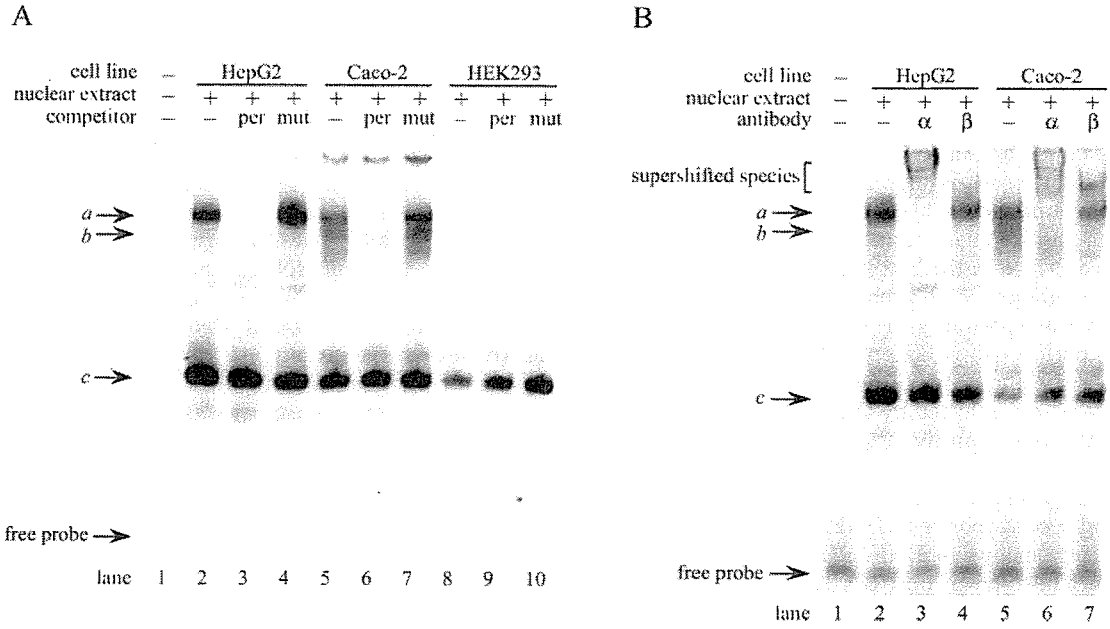

Fig. 6. Electrophoretic mobility shift assay using the oligonucleotide probe corresponding to the −76/−41 region and nuclear extracts from HepG2, Caco-2, and HEK293 cells. A, competition assays. Digoxigenin-labeled probe (Table 1) was incubated with nuclear extracts from HepG2, Caco-2, and HEK293 cells in the presence or absence of a 25-fold excess of unlabeled competitor (per or mut) as indicated. B, supershift analysis. The probe was incubated with nuclear extracts from HepG2 and Caco-2 cells in the presence or absence of a specific antibody against HNF1α (α) or HNF1β (β) as indicated. The DNA-protein complex was detected as described under *Materials and Methods*.

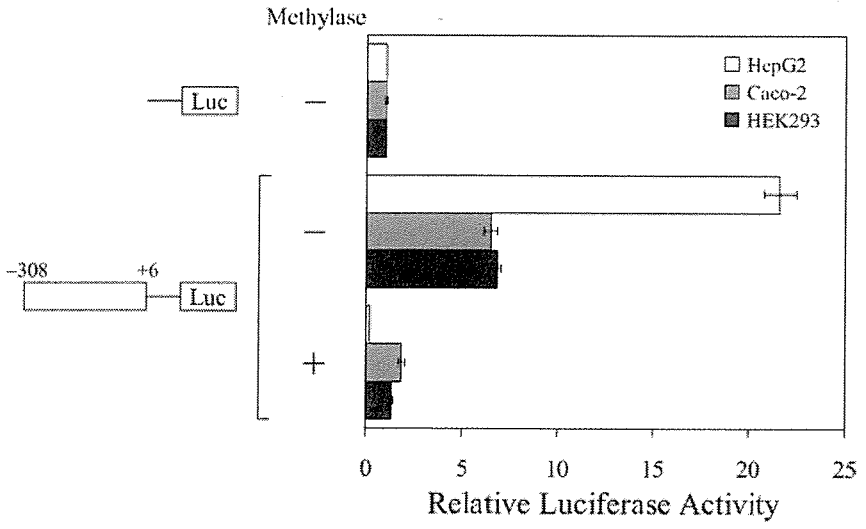

Fig. 7. Effect of in vitro methylation on the hOAT3 promoter activity. hOAT3 −308/+6 promoter construct was methylated in vitro with SssI methylase and transfected into HepG2 (white bars), Caco-2 (gray bars), and HEK293 cells (black bars). The luciferase activity was measured as described under *Materials and Methods* and was shown as the factor of induction over background activity measured in cells transfected with pGL3-Basic without methylation in each cell line. Results are presented as the mean ± S.E. of triplicate samples.

mined using a series of deleted promoter-reporter constructs (Fig. 2), and the region extending from −308 to +6 relative to the transcriptional start site was found to be important for promoter activity. An almost 70% homologous sequence over 300 base pairs to the hOAT3 minimal promoter was found in the mouse and rat Oat3 genomic locus. A database search with Mat Inspector revealed that the TATA motif and HNF1 motif are conserved among species as depicted in Fig. 1, suggesting the importance of these elements in the regulation of OAT3 genes.

The contribution of HNF1α and HNF1β to the basal promoter activity of the hOAT3 gene was demonstrated by several in vitro studies. Mutations in the hOAT3 minimal promoter HNF1 motif resulted in an approximately 50% reduction in the luciferase activity compared with the wild-type construct in HepG2 and Caco-2 cells, but not in HEK293 cells (Fig. 4), which is consistent with the different expression pattern of HNF1α and HNF1β in these cell lines (Fig. 3). The residual activity of the mutated construct may be ascribed to the transactivation by other factors, the binding of which is also affected by DNA methylation, because in vitro methylation of the minimal promoter construct almost abolished its activity (Fig. 7). The amount or contribution of these unknown factors in HEK293 cells may be higher than that in Caco-2 cells, because the luciferase activity of the hOAT3 minimal promoter in HEK293 cells is similar to that in Caco-2 cells regardless of the absence of HNF1α and HNF1β. Further studies will be required to identify these factors that are also required for the transcription of hOAT3. Cotransfection of HNF1α and/or HNF1β dramatically enhanced the hOAT3 wild-type promoter-driven luciferase activity in HEK293 cells, whereas the luciferase activity driven by the mutated promoter was unaffected (Fig. 5). Binding of HNF1α or HNF1β to the HNF1 binding motif in the hOAT3 promoter was confirmed by electrophoretic mobility shift assays (Fig. 6A). Supershift analysis using specific antibodies for HNF1α and HNF1β suggested that the protein complex binding to this region is HNF1α/HNF1α homodimer or HNF1α/HNF1β heterodimer (Fig. 6B). These data indicate that HNF1α, HNF1β, or both are critical for hOAT3 gene expression, although the transactivation potency of HNF1β is lower than that of HNF1α (Fig. 5). It seems that the transcription of mOat3 is also under the control of HNF1α and HNF1β. The involvement of HNF1α and HNF1β in regulation of the OAT3 gene is conserved among species, further supporting a critical role for these transcription factors in the regulation of the hOAT3 and mOat3 genes.

hOAT3 is predominantly expressed in the kidney and only weakly in the brain and skeletal muscle (Cha et al., 2001; Alebouyeh et al., 2003). Moreover, in the kidney, the expression is restricted to the proximal tubules. Consistent with the distribution of hOAT3 in the kidney, HNF1α expression is primarily detected in the proximal tubules, whereas HNF1β is expressed throughout all segments of the nephron, from the proximal tubules to the collecting ducts (Lazzaro et al., 1992; Pontoglio et al., 1996). However, it should be noted that the tissue distribution of HNF1α and HNF1β is much wider than that of hOAT3 (Blumenfeld et al., 1991; Rey-Campos et al., 1991). In addition to the kidney, they are expressed in the liver, intestine, stomach, and pancreas where hOAT3 is not expressed. Therefore, the tissue-specific and region-restricted expression of hOAT3 cannot be accounted for only by HNF1α and/or HNF1β, and other mechanisms must be involved in the regulation of hOAT3 expression.

Because multiple CpG dinucleotides are located in the hOAT3 minimal promoter region (Fig. 1), the involvement of DNA methylation in the regulation of hOAT3 expression was investigated. The transcriptional activity of the hOAT3 minimal promoter was suppressed by in vitro methylation of the reporter construct (Fig. 7). The expression of hOAT3, normally silent in Caco-2 and HEK293 cells, was activated de novo by DNA demethylation in Caco-2 cells, and by the transient transfection of HNF1α or cotransfection of HNF1α and HNF1β together with the DNA demethylation in HEK293 cells (Fig. 8). However, the expression of hOAT3 in HEK293 cells transfected with HNF1β alone followed by DNA demethylation with 5azadC was below the detection limit, although independent transfection of HNF1β enhanced the luciferase activity of hOAT3 wild-type reporter construct (Fig. 5). This could be due to the lower transactivation potency of the HNF1β/HNF1β homodimer. On the other hand, there was no induction of hOAT3 mRNA in HepG2 cells by 5azadC treatment, regardless of the presence of endogenous HNF1α and HNF1β. The lack of inducibility of hOAT3 expression in HepG2 may be accounted for by the presence of negative regulatory factors observed predominantly in HepG2 cells in the luciferase assays (Fig. 2) and/or the absence of other transcription factors necessary for de novo

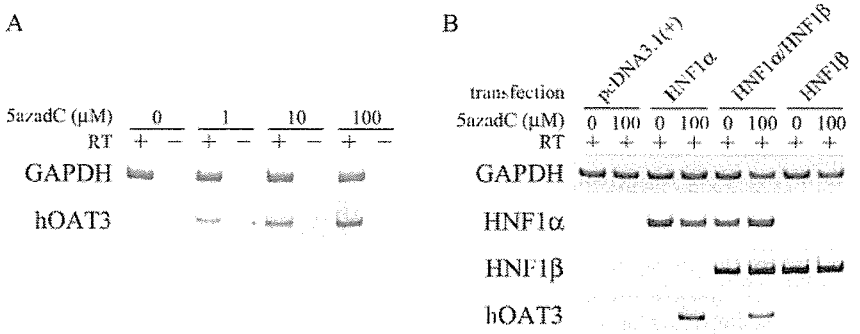

Fig. 8. Reactivation of the hOAT3 expression in hOAT3-negative cells. A, expression profile of hOAT3 mRNA in 5azadC-treated Caco-2 cells. The expression of GAPDH and hOAT3 mRNA was determined by RT-PCR in Caco-2 cells cultured for 72 h with 0, 1, 10, or 100 μM 5azadC. B, expression profile of hOAT3 mRNA in HEK293 cells transfected with HNF1α and/or HNF1β together with 5azadC treatment. The expression of GAPDH, HNF1α, HNF1β, and hOAT3 mRNA was determined by RT-PCR in HEK293 cells transiently transfected with 0.5 μg/well pcDNA3.1(+), 0.5 μg/well HNF1α, 0.25 μg/well HNF1α and HNF1β, or 0.5 μg/well HNF1β, followed by treatment with 0 or 100 μM 5azadC for 48 h. Results with the PCR templates with reverse transcription (RT +) are shown. No amplified products were detected from the templates without reverse transcription (data not shown).

expression of hOAT3. Further analysis will be required for the identification of these factors. Taken together, these observations indicate that the expression of hOAT3 is negatively regulated by DNA methylation.

There have been several reports regarding the involvement of DNA methylation in tissue-specific gene expression (Cho et al., 2001; Imamura et al., 2001; Futscher et al., 2002; Hattori et al., 2004; Jin et al., 2005). It is possible that the minimal promoter region of hOAT3 is hypermethylated in the tissues where the expression of hOAT3 is not detected, such as liver and intestine. The hypermethylation of the promoter region may render the neighboring chromatin structure inaccessible for many transcription factors, including HNF1α and HNF1β, through deacetylation of histones. Thus, regardless of the expression of HNF1α and HNF1β, the expression of hOAT3 is suppressed in those tissues.

The mechanism underlying the proximal tubule-restricted expression of hOAT3 in the kidney is more complicated. The nuclear extracts from the kidney normally contain HNF1α/HNF1β heterodimers and HNF1β/HNF1β homodimers (Pontoglio et al., 1996), and the results of the supershift experiments suggest that the protein complex binding to the HNF1 motif of hOAT3 might be the HNF1α/HNF1α homodimer or HNF1α/HNF1β heterodimer (Fig. 6B). It is likely that the promoter region of hOAT3 is hypomethylated in the kidney proximal tubules, enabling the HNF1α/HNF1β heterodimers to bind to their recognition sites. This model is supported by the results showing that the expression of hOAT3 was induced by cotransfection of HNF1α and HNF1β with the concomitant DNA demethylation in HEK293 cells (Fig. 8B). The methylation status in the other nephron segments is debatable. The promoter region may be hypermethylated in the whole nephron except for the proximal tubules, resulting in the suppression of hOAT3 expression. A second possibility is that although the promoter region is not highly methylated, interaction with the HNF1β/HNF1β homodimer is not sufficient to evoke the hOAT3 expression as observed in Fig. 8B.

Taking all these findings into consideration, it seems that the tissue specificity of the expression of hOAT3 may be explained by the coordinated action of genetic (HNF1α and HNF1β) and epigenetic (DNA methylation) mechanisms. Analysis of the Oat3 expression in HNF1α-null mice (Pontoglio et al., 1996; Lee et al., 1998) will show the relative contribution of HNF1α in vivo. In addition, direct demonstration of the difference in the DNA methylation and chromatin status in the hOAT3 promoter region among in vivo tissues/cells will be required in future studies.

The tissue distribution of mOat3 and rOat3 is not consistent with that of hOAT3: they are expressed not only in the kidney but also in the liver and the brain (Kusuhara et al., 1999; Kikuchi et al., 2003; Ohtsuki et al., 2004). It is noteworthy that the positions of the CpG dinucleotides in the hOAT3 promoter are not conserved in the corresponding region of mouse and rat Oat3 (Fig. 1). The difference in the contribution of epigenetic factors to the regulation of OAT3 gene expression may explain the species difference in the expression patterns, because the contribution of genetic factors seems to be comparable as far as HNF1α and HNF1β are concerned.

Despite the numerous studies of the genes regulated by HNF1α or HNF1β, there are few reports regarding the mechanism whereby these homeodomain proteins can bind to the promoter region of their target genes or transactivate the expression in a tissue-specific manner. Here, we have provided the first evidence suggesting that the methylation profile of the promoter or the chromatin configuration of the target genes determines the accessibility of HNF1α and HNF1β. The synergistic action of the chromatin structure in the promoter region and binding of HNF1α and HNF1β could be a critical clue to the further understanding of the tissue-specific gene regulation by these two transcription factors. Future studies are needed to investigate whether this scheme is applicable to other genes.

In conclusion, the present study provides a clear demonstration that the expression of hOAT3 is positively regulated by HNF1α and HNF1β and negatively regulated by DNA methylation. This is the first demonstration of the importance of HNF1α and HNF1β in the regulation of genes indispensable for detoxification in the kidney. Furthermore, it is also suggested that the coordinated action of genetic and epigenetic factors might explain the tissue-specific expression of hOAT3.

References

Alebouyeh M, Takeda M, Onozato ML, Tojo A, Noshiro R, Hasannejad H, Inatomi J, Narikawa S, Huang XL, Khamdang S, et al. (2003) Expression of human organic anion transporters in the choroid plexus and their interactions with neurotransmitter metabolites. *J Pharmacol Sci* **93:**430–436.

Bai Y, Pontoglio M, Hiesberger T, Sinclair AM, and Igarashi P (2002) Regulation of kidney-specific Ksp-cadherin gene promoter by hepatocyte nuclear factor-1beta. *Am J Physiol* **283:**F839–F851.

Barbacci E, Reber M, Ott MO, Breillat C, Huetz F, and Cereghini S (1999) Variant hepatocyte nuclear factor 1 is required for visceral endoderm specification. *Development* **126:**4795–4805.

Bird A (2002) DNA methylation patterns and epigenetic memory. *Genes Dev* **16:**6–21.

Blumenfeld M, Maury M, Chouard T, Yaniv M, and Condamine H (1991) Hepatic nuclear factor 1 (HNF1) shows a wider distribution than products of its known target genes in developing mouse. *Development* **113:**589–599.

Cha SH, Sekine T, Fukushima JI, Kanai Y, Kobayashi Y, Goya T, and Endou H (2001) Identification and characterization of human organic anion transporter 3 expressing predominantly in the kidney. *Mol Pharmacol* **59:**1277–1286.

Cheret C, Doyen A, Yaniv M, and Pontoglio M (2002) Hepatocyte nuclear factor 1 alpha controls renal expression of the Npt1-Npt4 anionic transporter locus. *J Mol Biol* **322:**929–941.

Cho JH, Kimura H, Minami T, Ohgane J, Hattori N, Tanaka S, and Shiota K (2001) DNA methylation regulates placental lactogen I gene expression. *Endocrinology* **142:**3389–3396.

Coffinier C, Gresh L, Fiette L, Tronche F, Schutz G, Babinet C, Pontoglio M, Yaniv M, and Barra J (2002) Bile system morphogenesis defects and liver dysfunction upon targeted deletion of HNF1beta. *Development* **129:**1829–1838.

Coffinier C, Thepot D, Babinet C, Yaniv M, and Barra J (1999) Essential role for the homeoprotein vHNF1/HNF1beta in visceral endoderm differentiation. *Development* **126:**4785–4794.

Eraly SA, Vallon V, Vaughn DA, Gangoiti JA, Richter K, Nagle M, Monte JC, Rieg T, Truong DM, Long JM, et al. (2006) Decreased renal organic anion secretion and plasma accumulation of endogenous organic anions in OAT1 knock-out mice. *J Biol Chem* **281:**5072–5083.

Futscher BW, Oshiro MM, Wozniak RJ, Holtan N, Hanigan CL, Duan H, and Domann FE (2002) Role for DNA methylation in the control of cell type specific maspin expression. *Nat Genet* **31:**175–179.

Gresh L, Fischer E, Reimann A, Tanguy M, Garbay S, Shao X, Hiesberger T, Fiette L, Igarashi P, Yaniv M, et al. (2004) A transcriptional network in polycystic kidney disease. *EMBO (Eur Mol Biol Organ) J* **23:**1657–1668.

Hasegawa M, Kusuhara H, Endou H, and Sugiyama Y (2003) Contribution of organic anion transporters to the renal uptake of anionic compounds and nucleoside derivatives in rat. *J Pharmacol Exp Ther* **305:**1087–1097.

Hasegawa M, Kusuhara H, Sugiyama D, Ito K, Ueda S, Endou H, and Sugiyama Y (2002) Functional involvement of rat organic anion transporter 3 (rOat3; Slc22a8) in the renal uptake of organic anions. *J Pharmacol Exp Ther* **300:**746–753.

Hattori N, Nishino K, Ko YG, Ohgane J, Tanaka S, and Shiota K (2004) Epigenetic control of mouse Oct-4 gene expression in embryonic stem cells and trophoblast stem cells. *J Biol Chem* **279:**17063–17069.

Imamura T, Ohgane J, Ito S, Ogawa T, Hattori N, Tanaka S, and Shiota K (2001) CpG island of rat sphingosine kinase-1 gene: tissue-dependent DNA methylation status and multiple alternative first exons. *Genomics* **76:**117–125.

Jin B, Seong JK, and Ryu DY (2005) Tissue-specific and de novo promoter methylation of the mouse glucose transporter 2. *Biol Pharm Bull* **28:**2054–2057.

Jung D, Hagenbuch B, Gresh L, Pontoglio M, Meier PJ, and Kullak-Ublick GA (2001) Characterization of the human OATP-C (SLC21A6) gene promoter and regulation of liver-specific OATP genes by hepatocyte nuclear factor 1 α. *J Biol Chem* **276:**37206–37214.

Kikuchi R, Kusuhara H, Sugiyama D, and Sugiyama Y (2003) Contribution of organic anion transporter 3 (Slc22a8) to the elimination of *p*-aminohippuric acid and benzylpenicillin across the blood-brain barrier. *J Pharmacol Exp Ther* **306:** 51–58.

Kusuhara H, Sekine T, Utsunomiya-Tate N, Tsuda M, Kojima R, Cha SH, Sugiyama Y, Kanai Y, and Endou H (1999) Molecular cloning and characterization of a new multispecific organic anion transporter from rat brain. *J Biol Chem* **274:**13675–13680.

Lazzaro D, De Simone V, De Magistris L, Lehtonen E, and Cortese R (1992) LFB1 and LFB3 homeoproteins are sequentially expressed during kidney development. *Development* **114:**469–479.

Lee YH, Sauer B, and Gonzalez FJ (1998) Laron dwarfism and non-insulin-dependent diabetes mellitus in the Hnf-1alpha knockout mouse. *Mol Cell Biol* **18:**3059–3068.

Lowry OH, Rosebrough NJ, Farr AL, and Randall RJ (1951) Protein measurement with the folin phenol reagent. *J Biol Chem* **193:**265–275.

Mendel DB and Crabtree GR (1991) HNF-1, a member of a novel class of dimerizing homeodomain proteins. *J Biol Chem* **266:**677–680.

Mendel DB, Hansen LP, Graves MK, Conley PB, and Crabtree GR (1991) HNF-1 alpha and HNF-1 beta (vHNF-1) share dimerization and homeo domains, but not activation domains, and form heterodimers in vitro. *Genes Dev* **5:**1042–1056.

Ohtsuki S, Kikkawa T, Mori S, Hori S, Takanaga H, Otagiri M, and Terasaki T (2004) Mouse reduced in osteosclerosis transporter functions as an organic anion transporter 3 and is localized at abluminal membrane of blood-brain barrier. *J Pharmacol Exp Ther* **309:**1273–1281.

Pontoglio M, Barra J, Hadchouel M, Doyen A, Kress C, Bach JP, Babinet C, and Yaniv M (1996) Hepatocyte nuclear factor 1 inactivation results in hepatic dysfunction, phenylketonuria, and renal Fanconi syndrome. *Cell* **84:**575–585.

Pontoglio M, Prie D, Cheret C, Doyen A, Leroy C, Froguel P, Velho G, Yaniv M, and Friedlander G (2000) HNF1alpha controls renal glucose reabsorption in mouse and man. *EMBO (Eur Mol Biol Organ) Rep* **1:**359–365.

Rey-Campos J, Chouard T, Yaniv M, and Cereghini S (1991) vHNF1 is a homeoprotein that activates transcription and forms heterodimers with HNF1. *EMBO (Eur Mol Biol Organ) J* **10:**1445–1457.

Robertson EE and Rankin GO (2005) Human renal organic anion transporters: characteristics and contributions to drug and drug metabolite excretion. *Pharmacol Ther* **109:**399–412.

Sekine T, Miyazaki H, and Endou H. 2006. Molecular physiology of renal organic anion transporters. *Am J Physiol* **290:**F251–F261.

Shih DQ, Bussen M, Sehayek E, Ananthanarayanan M, Shneider BL, Suchy FJ, Shefer S, Bollileni JS, Gonzalez FJ, Breslow JL, et al. (2001) Hepatocyte nuclear factor-1alpha is an essential regulator of bile acid and plasma cholesterol metabolism. *Nat Genet* **27:**375–382.

Shiota K (2004) DNA methylation profiles of CpG islands for cellular differentiation and development in mammals. *Cytogenet Genome Res* **105:**325–334.

Sweet DH, Miller DS, Pritchard JB, Fujiwara Y, Beier DR, and Nigam SK (2002) Impaired organic anion transport in kidney and choroid plexus of organic anion transporter 3 (*Oat3* (*Slc22a8*)) knockout mice. *J Biol Chem* **277:**26934–26943.

Tronche F and Yaniv M (1992) HNF1, a homeoprotein member of the hepatic transcription regulatory network. *Bioessays* **14:**579–587.

Van Aubel RA, Masereeuw R, and Russel FG (2000) Molecular pharmacology of renal organic anion transporters. *Am J Physiol* **279:**F216–F232.

Address correspondence to: Dr. Yuichi Sugiyama, Department of Molecular Pharmacokinetics, Graduate School of Pharmaceutical Sciences, The University of Tokyo, 7-3-1 Hongo, Bunkyo-ku, Tokyo 113-0033, Japan. E-mail: sugiyama@mol.f.u-tokyo.ac.jp